BILINGUAL PUBLISHING CO.
Pioneer of Global Academics Since 1984

01
2020

Journal of Geological Research

Volume 2 | Issue 1 | January 2020 | ISSN 2630-4961 (Online)

ISSN 2630-4961
01
9 772630 496201

Volume 2 Issue 1 • January 2020 • ISSN 2630-4961 (Online)

Journal of Geological Research

Editor-in-Chief

Professor. Dr. Sayed Hemeda

BILINGUAL PUBLISHING CO.
Pioneer of Global Academics Since 1984

Volume 2 | Issue 1 | January 2020 | Page 1-42
Journal of Geological Research

Contents

Article

BILINGUAL PUBLISHING CO.
Pioneer of Global Academics Since 1984

Journal of Geological Research
https://ojs.bilpublishing.com/index.php/jgr-a

ARTICLE

Geomorphological Evolution and Palaeoenvironmental Change in the Western Alashan Plateau, China

Bingqi Zhu*

Key Laboratory of Water Cycle and Related Land Surface Processes, Institute of Geographic Sciences and Natural Resources Research, Chinese Academy of Sciences, Beijing, 100101, China

ARTICLE INFO

Article history
Received: 1 June 2020
Accepted: 25 June 2020
Published Online: 30 June 2020

Keywords:
Relic Landform
Geomorphic processes
aeolian-fluvial interaction
Late Pleistocene
Holocene
Western Alashan

ABSTRACT

Although neotectonic activity is considered to be the main factor of the terrain evolution of the Qinghai Tibet Plateau and its surrounding high-altitude areas, further geomorphological analysis and literature analysis are needed for the understanding of the geomorphic evolution and the Quaternary environment change of the western area of the Alxa Plateau near the northern Tibet Plateau. The purpose of this study is to investigate the distribution of site-specific geomorphic units of the landforms developed in the vast topography of Ejina Basin (Western Alxa), in order to identify the geostructural and climatic causes of the geomorphic landscape and its impact on the change of paleoenvironment. At present, the climate and hydrological conditions in Ejina are relatively monotonous and stable. In addition to tectonic dynamic factors, the most widely distributed landform in the basin is climate landform. There are both geomorphological and sedimentological anomalies of Aeolian landforms occurred in the whole basin, indicating that the underlying surface effect (retention effect) of river (Ejina River) and its related uneven ground and weak wind erosion (deflation) process in the nearby area may be the important factors controlling the formation of Ejina dunes, rather than the arid climate. It is believed that the extensive interaction between the aeolian and fluvial processes is the main mechanism of the regional geomorphic difference in Ejina Basin. According to the comparability of regional geomorphology and sedimentology, the period of the formation of relic geomorphology in the edge of Ejina Basin can be reasonably attributed to the local glacial maximum of the last glacial. The geomorphic transformation from quasi plain and desert valley to desert plain, the appearance of widely moving sand dunes and the presence of large ancient lake geomorphology all indicate that the drought index of Ejina Basin is increasing on the scale of geomorphic formation. Paleogeomorphological and chronological evidences show that the climatic and hydrological conditions of the basin in the last glacial period and the early Holocene are much better than those at present. For example, the average annual precipitation in the area before 39-23ka BP is between 60-350 mm (about 36 mm today), but there are large waves in the Holocene. The coexistence of various climates and landforms in Ejina Basin and the resulting geomorphic diversity should be the composite result of various geomorphic processes and surface processes besides glaciation. The low aridity (relative humidity) in the Ejina Region in the late Pleistocene may be the result of the enhancement of the westerly rain belt and the weakening of the Asian Winter Monsoon in the arid region of Central Asia.

**Corresponding Author:*
Bingqi Zhu,
Key Laboratory of Water Cycle and Related Land Surface Processes, Institute of Geographic Sciences and Natural Resources Research, Chinese Academy of Sciences, Beijing, 100101, China;
Email: zhubingqi@igsnrr.ac.cn

 DOI: https://doi.org/10.30564/jgr.v2i1.1942

1. Introduction

It is of great significance to understand the climatic history of the desert landforms in the late Quaternary in China for understanding the airfification/aridity of the interior of Central Asia and the evolution of the East Asian monsoon climate and the westerly climate systems [1-17]. At present, the distribution of arid areas in China can be expressed by annual precipitation. The extremely arid (< 100 mm) and arid areas (100-250 mm) are distributed in the central-northern and northwestern regions of China, while the semi-arid areas (250-500 mm) are mainly distributed in the east-northern regions (Figure 1). However, during the late Quaternary, China's sandy deserts and desert areas were affected by the infiltration of monsoon climate and the related significant increase of humidity, and many of them were in the transition between the eolian and the lacustrine environment [7,18-20], leading to great changes of the general arid environment in northern China. Large deserts such as Badanjin Desert and Taklimakan Desert and the lake water levels in these desert basins have made obvious response to the environmental changes from early to middle Holocene, especially the changes of intensity and precipitation/evaporation rate of the westerlies [7,19]. Therefore, China's deserts and desert margins are highly sensitive to climate change.

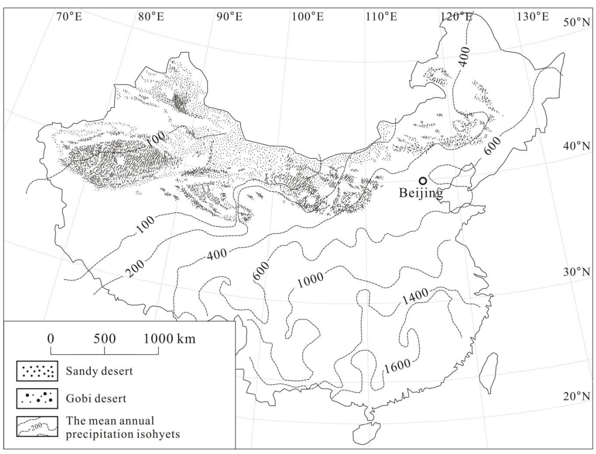

Figure 1. Distribution of the deserts and the annual mean precipitation in China

At present, China has only carried out extensive environmental monitoring on a small portions of desert areas, and the basic environmental information in most desert areas is often incomplete, or even can not be obtained at all [21]. At present, the available clues reflecting the environmental history of China's desert areas are largely derived from the evidences of loess and paleosol sedimentary sequences in desert margins or remote areas [3, 13-14, 22-23]. Limited by these data being not available, it is difficult to assess the impact of current environmental change and understand how the desert system can cope with past climate change. A more comprehensive understanding of these desert environmental systems requires extensive use of new methods and approaches to characterize and monitor deserts in China [21].

There is an academic term in geomorphology, named "geomorphodiversity", which was proposed and defined by Panizza [24] and Testa et al. [25]. It is an important evaluation method for geomorphic characteristics and geomorgenetic dynamics of a landform. This concept draws on similar and well-known terms of "biodiversity" and less well-known terms of "geodiversity" [26]. Based on these two disciplines, a new term in climate science, "climatediversity" has recently been proposed by the climate academia [27]. Due to the rapid development of the earth system science, the geological and climatological circles are now actively emphasizing on a new comprehensive science integrating "biodiversity", "geodiversity" and "climatediversity" [27], in which "geomorphodiversity" is regarded as an important component. It is defined as a discipline to identify the complexity and diversity of different geomorphic types of landform units under different environmental conditions and to explain the related geomorphogenic mechanism. From this point of view, valuable information can be obtained from different geomorphogenetic landforms through reasoning and hypothesis, so as to better understand the geomorphic factors driving the formation of current geomorphology. From this point of view, valuable information can be obtained from different geomorphogenetic landforms through geomorphic classification, similarity reasoning and hypothesis, so as to better understand the potential factors driving the formation of current landforms.

On the Mongolian Plateau in Central Asia, there are more than 1.3 million square kilometers of Gobi (stone) deserts, which are composed of wide and shallow basins. The smooth rock particles on the ground surface of these deserts are filled with sand, silt/clay, pebble or more common gravel [28]. These Gobi desert landscapes, especially the Alashan Plateau and its surrounding deserts, are considered as the main sources of dust emission in Central Asia [29-31]. Ejina Basin, located in the west of Alashan Plateau, is the center part of the Gobi desert belt in the Mongolia Plateau, and also the closed end area of the Heihe River Basin, the second largest inland river basin in China (Figure 2). In terms of climatology, Ejina Basin is located in the northern margin of the low-altitude Asian Summer Monsoon and also in the latitude ranges of the high-altitude westerlies (Figure 3). Therefore, the basin has potential significance for understanding global climate change

  DOI: https://doi.org/10.30564/jgr.v2i1.1942

and the response of plateau region to climate change. Tectotically speaking, the Alashan Plateau is an ancient stable block, but it has become active since Mesozoic [22]. The geomorphic and environmental evolution of the area is influenced by the tectonic stages caused by the compression of Eurasian, Indian and Pacific plates. Therefore, the study of geomorphology and paleoenvironment of the area also provides evidence for the study of the environmental impact of the uplift of the Qinghai-Tibet Plateau and the formation of the East Asian Monsoon [22, 32]. Up to now, however, there are few documents about the evolution of geomorphology and Paleoenvironment in the Ejina Basin. This paper is devoted to the geomorphic study of desert landscapes in the Alashan Plateau in northern China, in order to get a new understanding of the geomorphodiversity of Ejina Basin and its related late Quaternary climate change.

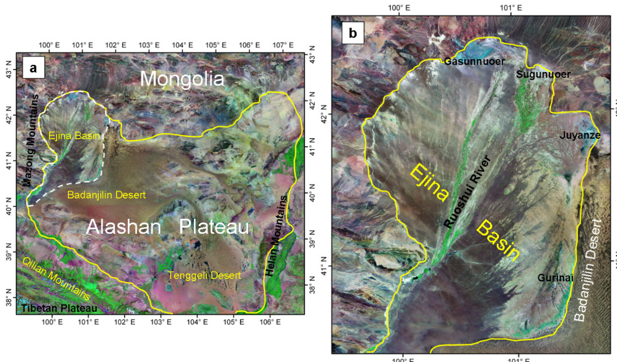

Figure 2. Overview remote-sensing images (Landsat TM, RGB 7-4-2) of the Alashan Plateau (a) and the Ejina Basin (b) (Cited from Zhu et al., [34]).

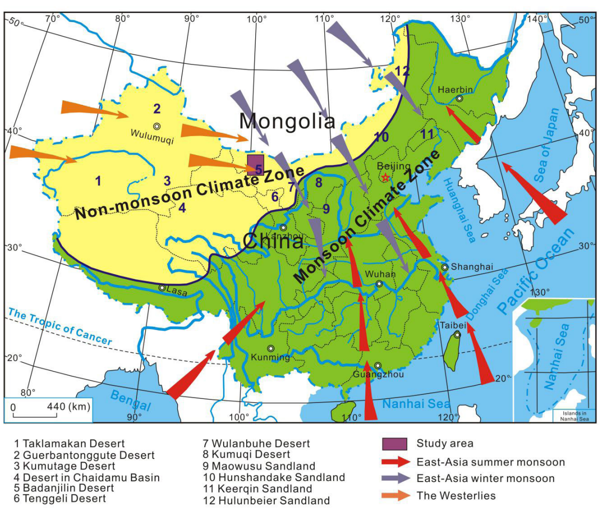

Figure 3. Distribution of deserts, monsoon zone and non-monsoon zone in China and the location of the Ejina Basin (modified from Zhu et al., [34])

2. Regional Setting and Methods

The Ejina Basin is located in the west part of the Alashan Plateau, between 40-43 ° N and 99-102 ° e (Figure 2, 3). The gravel plain of the Alsshan Gobi and the big sand sea of the Badanjilin Desert are adjacent to the basin in the north and East respectively (Figure 2). The Ejina basin is composed of three main sub-basins. When the Ejina River moves back and forth on its tail delta, these sub-basins are supplied by the river alternately. From west to East, these basins are the Gashunor Basin, the Sugunor Basin and the Juyanze Basin (Figure 2b).

At present, the climate of the Alashan Plateau belongs to extreme arid climate, with single hydrological environment. Only one river system (the Ejina River) is developed in the Ejina Basin [33]. The climate of Ejina Basin belongs to arid climate under desert conditions. In the past 50 years, the average annual temperature of Ejina is 8.8 ℃ (Figure 4a), the maximum daily temperature is 41 ℃ (July), and the minimum temperature is - 36.4 ℃ (January). The annual average precipitation of the last 50 years recorded by the Ejina meteorological station is 35.6mm (Figure 4a). From the perspective of climate, the region can be divided into extreme drought (120 > P > 60mm) or drought (60 > P > 30mm) according to different sub-regions (perucca and Martos, 2012). The multi-year average prevailing wind comes from the west, and the northwest wind is almost common from August to September on the annual scale.

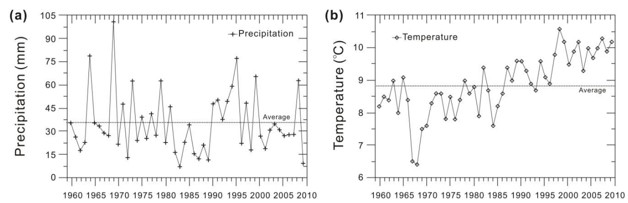

Figure 4. Variations of the average annual precipitation and temperatures (over 50 years during AD 1960-2010) in the Ejina Basin

In order to build a comprehensive database of geomorphological and climatic analysis in the Ejina Basin, we need to integrate data sets from wide different disciplines and use the technology of image processing and geographic information system (GIS) and the tools of spatial statistical analysis. Among these data sets, the geochronological analysis database (such as OSL and 14C dating data) comes from the domestic and foreign literatures on desert Research in China. Zhu et al. [34] conducted a geomorphological field survey in the whole Ejina Basin and partially described it. According to Landsat-ETM+ image data, topographic map and field investigation, they described

DOI: https://doi.org/10.30564/jgr.v2i1.1942

the geomorphological pattern of the basin and the geomorphological characteristics of special landforms in different types on different spatial scales in the Ejina Basin. They studied the sedimentary facies and shallow surface sedimentary profile in the middle, south and north parts of the Ejina Basin, and found out the specific combination of genetic related sedimentary facies, which provided the basis for the interpretation of sedimentary environment. For a detailed review of selected natural geomorphic elements, thematic maps of 1:500000 scale, topographic maps of 1:100000 scale and aerial and satellite photographs were used. Global positioning system (GPS) and Google Earth 1:50000 images were also used for field positioning. This paper focuses on the identification and investigation of the modern morphogenetic processes in the Ejina Basin, which is 980-2500 meters above sea level. The upper, middle and lower reaches of the Ejina River flowing from Langxinshan northwards to the Lake Sugunor (East Juyan sea) are investigated in detail. The geomorphological recognition and classification of landforms are mainly based on the system and principle of climate Geomorphology (for some details, see the literature [34-35]). In the research work, the records of precipitation, temperature and wind on the annual, monthly and daily scales from 1960 to 2010 were collected from the Ejina meteorological station (subordinate to the Ejina Qi Meteorological Bureau) in the middle part of the Ejina Basin, which was used to explain the potential climatic and geomorphic processes or geomorphic background. In addition, combining with modern meteorological data of the Ejina Basin in recent decades, we have adopted some geomorphoclimatic models buildted from the principles of climatic geomorphology to identify the modern dominant geomorpholodynamics and related geomorphic processes occurred in the Ejina Basin. On the basis of this, the environmental indications of the modern and ancient climatic landforms in the Ejina Basin and the law of landform evolution are discussed.

3. Results and Discussion

3.1 Tectonic and Climatic Landforms in the Ejina Basin

Based on the major geomorphic types and geological structure, as well as the degree of structural stability, the application of geomorphic standards in deserts can generally be divided into shield / platform deserts and mountain / basin deserts [36]. Shield desert is basically formed on cratonic terrane, which is basically formed by late Precambrian rocks and platforms with young age. They are characterized by flat terrain and are damaged by recent volcanic mountains and important faulting activities. Mountain deserts are usually made up of long-distance mountain groups separated by lowlands [36]. According to this definition, the Alashan Plateau deserts belong to mountain/basin desert. They are the marginal landforms of some highlands formed during the Mesozoic and Cenozoic alpine orogeny [37]. Due to the topographical contrast and terrain difference, the high altitude areas are continuously eroded, and the formed materials are deposited in the form of coalescence alluvial fans in the depression lowlands or basins, such as the Ejina Basin (Figure 2).

Quantitative geomorphic information of the Alashan Plateau was previously extracted by researchers from digital elevation model [19,34,37]. These studies reveal that the geomorphic types of landforms in the Alashan Plateau are neither uniform nor homogenic and there are systematic regional differences in the plateau, but on the whole, it presents a topographical pettern of south-higher-than-north and east-higher-than-west. Most areas of the plateau are characterized by positive terrain, that is, the terrain with positive correlation between elevation and relief, and average slope. Based on radar wave data and Landsat Image (TM, MSS) data, many ancient hyrological landforms such as river valleys and lake basins buried by aeolian sands were identified in the north of the Ejina Basin and the Alashan Plateau [37]. The ancient hyrological system is in a NW-SE trend, which is obviously not in line with the present geomorphic pattern of south-higher-than-north and east-higher-than-west. This fact indicates that the neotectonic movement since Pleistocene may have caused a severe relief reversal in the Alashan Plateau.

On the Alashan Plateau, the topographical change in the Ejina Basin, especially along the Ejina River, is the largest in the whole plateau, because they span the margin zone of an ancient eroded plateau. This means that the topography of Ejina Basin is strongly controlled by the regional tectonic background. Except for the Ejina Basin, there is no continuous fluvial process in any other area of the Alashan Plateau (only confluence process of transient water flow and other hydrological processes exist locally, [33]). This means that the current climatic and hydrological conditions in the Ejina Basin are relatively special, monotonous and stable under the plateau background. They constitute the main geomorphological processes and geomorphic forces of the Ejina Basin. Based on this point, we believe that the river system evolution at basin scale, the efficiency of water and sediment transport, the ability of river to transport sediments out of the Qilian Mountain, coupled with the large-scale climate change and tectonic-controled topography, are the main mechanisms to explain the geomorphic differences in the Ejina Basin. It can be said that the process of basin sediment filling caused by

DOI: https://doi.org/10.30564/jgr.v2i1.1942

low efficiency of runoff conditions is smoothing and eliminating the tectonical relief of mountain desert system, which is the general trend of landform evolution in the Ejina Basin. On the other hand, it should be noted that the current smoothing model starts at the same time with the tectonic contrstuction of the basin relief. The current geomorphic evolution of the Qilian Mountains in the northeast of the Qinghai Tibet Plateau is the clearest illustration of this model [34].

Therefore, in terms of geomorphology, the topographic conditions of the Ejina Basin are diverse due to the coexistence of mountains, peneplain and basins, which are directly related to the formation of geomorphology related to geological processes such as structure, erosion, transportation and sedimentation [33-34]. We can emphasize that the first-class landform of the basin is determined by regional lithologic geology and structural factors, which are obvious structural geomorphic dynamic process, showing obvious topographic gradient and terrain difference between the Qilian Mountain in the south, the Mazong Mountain in the West and the lake facies base basins in the East and the North (Figure 5).

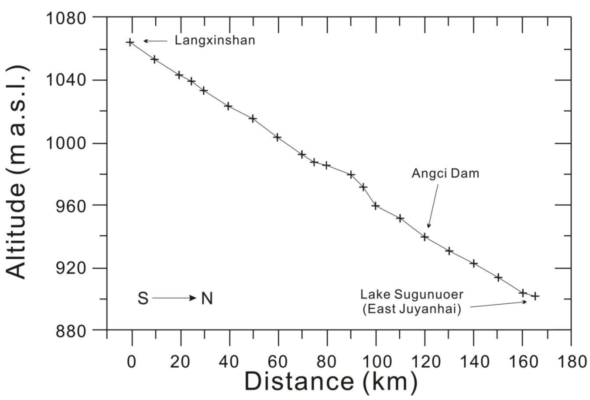

Figure 5. A topographical profile of the S-N trending line along the Ejina River from Langxinshan to Lake Sugunuoer

In addition to morphotectodynamic factors, satellite images and field investigations show that the Ejina Basin is located in the center of the arid area in northern China. Desert landscapes such as Gobi and aeolian sand dunes are the most widely distributed landforms here and even in northern China, which are obviously the fruit of climate factors, and therefore the most typical types of climate-driven landforms [6-7, 34, 38-40]. In terms of climate geomorphology, the climate-driven landforms occurred in the Ejina Basin can be roughly divided into six types.

Desert plain, also known as "Gobi" or "gravel desert", is a kind of landform controlled by aeolian dynamics and water dynamics and the interaction intensity between the two dynamics is relatively equal. In terms of climate geomorphology, it is a typical landform with balance of wind and water forces [38]. The energy of the geomorphodynamics that forms desert plain is usually low and the ideal precipitation required to form the landform is between 30-60 mm [38]. Landforms of desert plain can be divided into two geomorphological types: the erosion-born type and the accumulation-born type. The accumulation type is close to the force of wind dynamics and the erosion type trends to the waterdynamics, such as peneplain or piedmont area [38-39]. The typical landform of desert plain is distributed in a large area of the whole Ejina Basin from south to north (Figure 6). It is also known as the "Great Central Gobi" or "the Ejina Black Gobi". The landform of desert plain in the Ejina Basin is mainly an accumulation-born type.

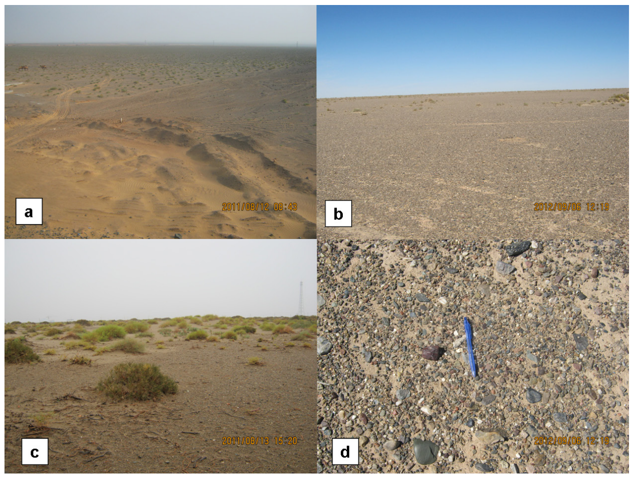

Figure 6. Landform of desert plains in the Ejina Basin

Pediment, one kind of the peneplain landform, is also a kind of landform in climatic origin [35]. It is a conical relief characterized by a channel net, namely a landform being gently inclined with cone-shaped plane that characterized by the distribution of river grids on the slope. The formation of pediment is mainly controlled by the frost weathering and periglacial (ice-margin) processes [38,41]. Pediment landform can be divided into two subtypes, the erosion-born type and the accumulation-born type, which usually occurs in piedmont and the front highland of desert plain [38]. The climate conditions for forming pediment are cold climate with annual mean temperature < - 3 ° C and annual mean precipitation between 150-300 mm [38]. The key to the formation of pediment is to produce loose rock debris through the freeze-thaw and weathering processes, and the precipitation converges into slope flow and then transports these clastic sediments to river channel or the front of alluvial fan for deposition [35,38]. The pediment landforms are mainly distributed in the western and northern edges of the Ejina Basin, the areas with higher eleva-

DOI: https://doi.org/10.30564/jgr.v2i1.1942

tion of piedmonts and desert plains (Figure 7).

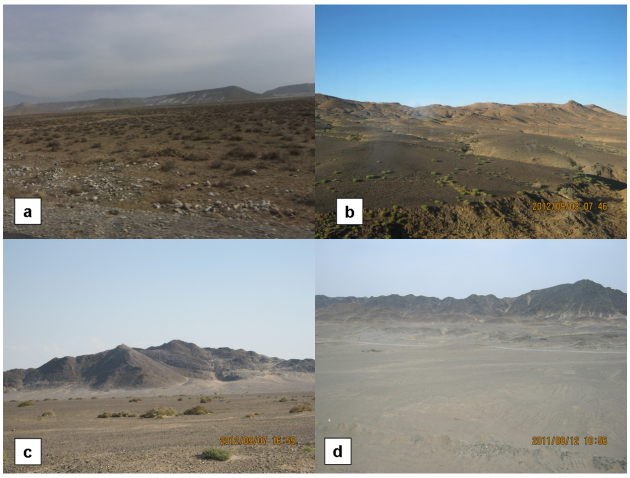

Figure 7. Landform of pediments in the Ejina Basin

Desert gorge or desert hill, is a landform which usually appears in the upper part of desert plain or piedmont. It is also a kind of climate landform formed by the transformation of tectonical landforms experienced the erosion and planation effects of the freeze-thaw, glacial and fluvial processes [38,41]. The environmental conditions for the formation of desert gorges are under the comprehensive effects of frost weathering and glaciation or fluvial processes, with annual mean precipitation between 100-300 mm [35,38]. The landform of desert gorges is widely distributed on the surrounding hillsides of the Mazong Mountains in the west of the Ejina Basin (Figure 8).

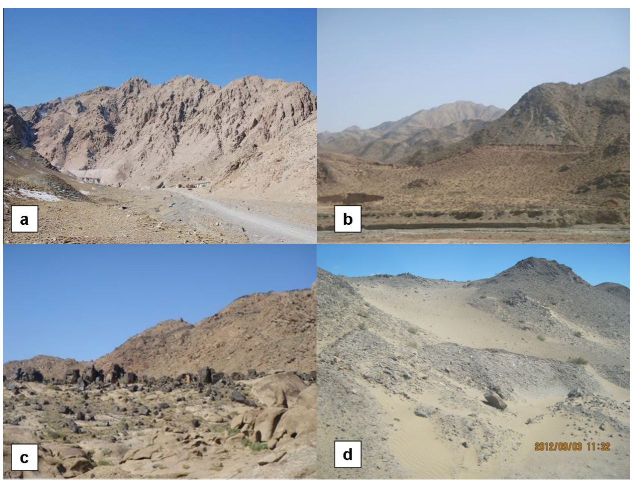

Figure 8. Landform of desert gorges in the Ejina Basin

Sandy dunes. In terms of climate geomorphology, sandy dune is a typical aerodynamic relief and an accumulation landform usually formed under arid environment with annual mean precipitation of less than 100 mm [35]. The main geomorphic forces forming this landform are wind (airflow or circulation), including aeolian (accumulation) and deflation (erosion) processes [38]. Therefore, sand dunes are regarded as a typical type of climate-driven landform [35]. Based on the theory of aeolian geomorphology, the formation of sandy dune landform in desert landscape is mainly controlled by several environmental factors. One is the stratification instability of the atmospheric boundary layer (i.e. the instability of troposphere thickness, the activity of near-groundsurface wind regime, and the high wind power or wind speed for sand-particle rising), the second is the foehn effect of dry radiabatic downdraft (i.e. drought conditions), the third is sufficient supply of sediment sources (sandy sediment availability), and the fourth is the uneven underlying surface conditions (a depositional environment of sediment accumulation rather than sediment erosion as formed by obstacles, so that sand dunes can be preserved). Identifying these factors is key to understand the formation of dune landform in desert landscape. The sand dune landform in the Ejina Basin is mainly distributed near the banks of the Ejina River (Figure 9), surrounded by Gobi (Figure 10). According to the vegetation-cover conditions, the dunes in the Ejina Basin can be divided into three sub-types: mobile dunes, semi-fixed dunes and fixed dunes (Figure 11). Populus euphratica, Tamarix, Artemisia, Hippophae rhamnoides and other plants are rarely distributed on the surface of sand dunes (Figure 9-11). Field investigation shows that the height of sand dunes changes regularly on the local scale, but the types of sand dunes in different places have little difference [33]. These three dune types are widely distributed and exist in any place of the basin.

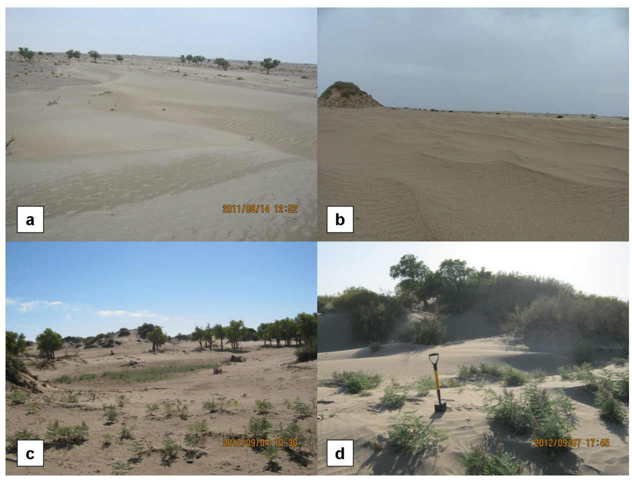

Figure 9. Aeolian landform (dune fields) in the Ejina Basin. (a) Single dunes and dune chanins, (b) sandy sheets, (c) and (d) Dunes accompanied by Tugai forests (Populus euphratica) and shrub vegetations (e.g., Chionese tamarisk) along the Ejina river banks

DOI: https://doi.org/10.30564/jgr.v2i1.1942

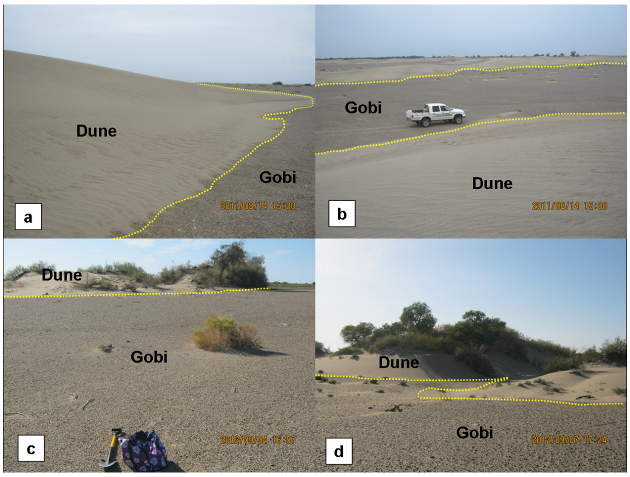

Figure 10. Active dunes developed on the Gobi deserts

Figure 11. Dune types in the Ejina Basin. (a) Active dune, (b) semi-active dune and (c) fixed dune

Fluvial and alluvial/proluvial landforms. These are typical hydrogenetic landforms controlled by river hydrodynamics and the hydroclimatic conditions of the drainage system. On the Alashan Plateau, the fluvial landform only exists in the Ejina Basin [34], but the temporary alluvial/proluvial landforms occur in the pediment areas which locate widely in the northern Ejina Basin and the northern Alashan Plateau. In addition to the existence of modern river channels (Figure 12), many ancient river channels and alluvial fans can still be identified in the central part of the Ejina Basin from field invetigations, historical maps and satellite images (Figure 2a). The Ejina River, also known as "Ruoshui River", belongs to the lower reaches of the Heihe River, the second largest inland river of China, and is a unique river flowing through the Ejina Basin. The river originates from the Qilian Mountains and emerges at the Ejina Basin from its south corner (Langxinshan). The Ejina River runs northward about 160 kilometers and finally flows into the Sugunor Lake (also known as the East-Juyan-Sea) at the north end of the basin (Figure 5). As the general relief of the Ejina Basin is flat and wide relative to that of the Heihe River catchment, the area of alluvial/proluvial landforms in the Ejina Basin is generally smaller than other areas of the Heihe River Basin.

Figure 12. Fluvial landforms in the Ejina Basin. (a) A satellite image of the river channel (East River), gobi and dune distribution on a short section in the central part of the Ejina basin (form Google Earth), (b) wide and flat river channel (no water flowing by at the time), (c) sandy sedimentation in the riverbed, (d) intermittent flood discharge with muddy water derived from the Qilian Mountains

Lacrustrine plain and playa landforms. No matter the alluvial/proluvial fan landform or lacustrine (lake) plain landform, they are all formed under the environment with better hydrological conditions. The formation of these landforms reflects that the initial climate is relatively humid and the river system is developed and the flood events are frequent. The landform of lacustrine plain is formed under the depositional environment with active water dynamics, while alluvial/proluvial fan is formed under the environment with static water dynamics. In the north of the Ejina Basin and the low reaches of the Ejina River, modern lake and playa basins are widely distributed (Figure 13). While in strata of the eastern and central Ejina Basin, deep lacustrine and marsh sedimentary layers are widely distributed, suggesting that lacustrine plain landforms existed in a large area of the Ejina Basin in the past. However, in the modern environment, the Ejina Basin has no hydroclimatic conditions for forming natural alluvial/proluvial plain and lacustrine plain, because the natural hydrological system has disappeared in the Ejina Basin and replaced by an artificially engineering hydrological system [34].

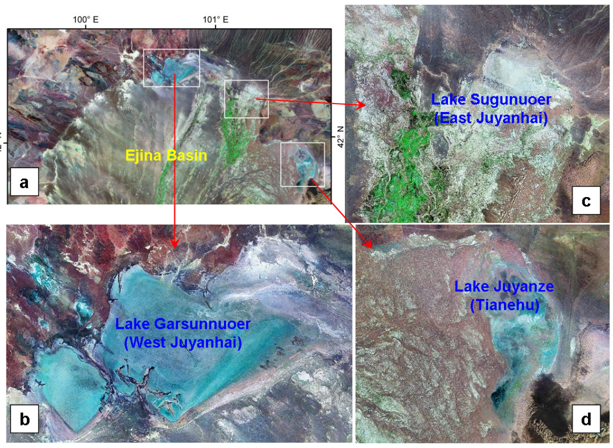

Figure 13. Overview remote-sensing images (Landsat TM, RGB 7-4-2) of the north part of the Ejina Basin (a), and the Lake Garsunnuoer (b), the Lake Sugunuoer (b) and the Lake Juyanze (d) in the Ejina Basin

3.2 Modern Geomorphodynamics and Morphoclimatic Processes in the Ejina Basin

In terms of climate geomorphology, there are many geomorphic models based on the theory of climate geomorphology, such as the Peltier model [42]. Combined with regional meteorological data, these models can be used to identify the relative importance of the main geomorphic dynamics and related geomorphological processes in an area. Peltier [42] uses the annual average temperature and rainfall data to define the semi-quantitative areas of frost/freezing strength and chemical weathering intensity, so as to define the frost and weathering dynamics and processes, respectively, as well as other dynamics such as gravity, glaciation, wind, pluvial erosion, fluvial and alluvial forces, etc., as shown in Figures 14-15. It has been reported that the simulated ranges of diverse geomorphodynamic regions superimposed on Peltier model map can prove the relative effectiveness of various geomorphic processes in arid and semi-arid environments, such as Mabbutt [36] and Gutierrez [35].

Applying the Peltier model to meteorological data such as annual mean temperature and precipitation over the past 50 years in the Ejina Basin, the Peltier model diagram states that:

The geomorphological system of the Ejina Basin is a geomorphoclimatic system from semi-arid type (less precipitation and moderate to warm) to arid type (less precipitation and cold to hot) types, which is dominated by physical processes and strong seasonality (Figure 14-15).

More than ten types of geomorphoclimatic forces that are common and recognizable in the world are distributed in Ejina Basin are as follows: the frost-freeze weathering

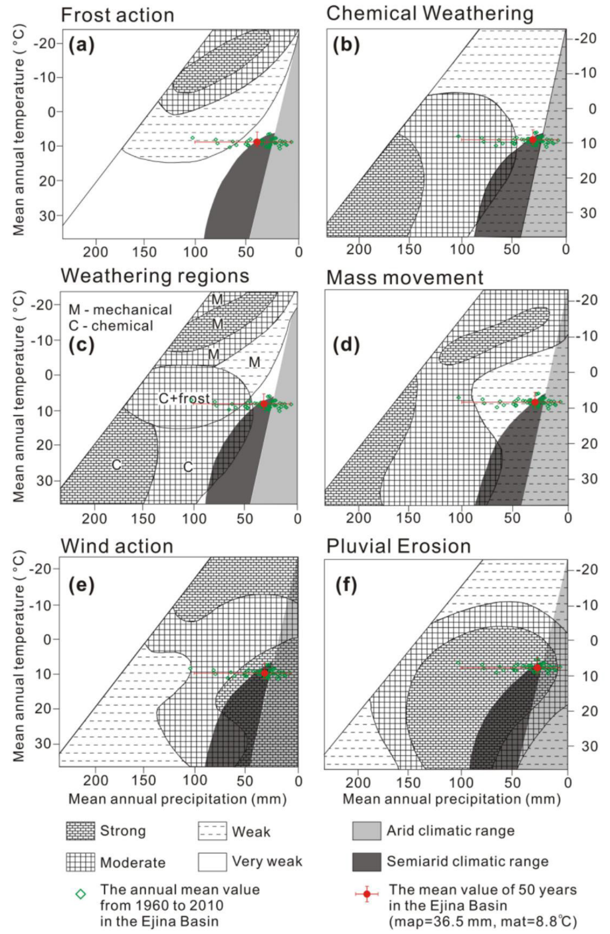

Figure 14. Effectiveness of landforming processes under different climatic conditions, related to arid and semiarid morphogenic regions. The basegraphs were after Peltier [42]

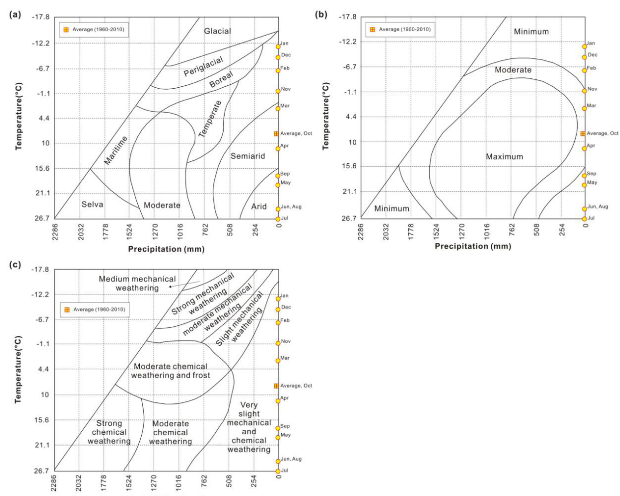

Figure 15. The affiliation of the characteristic months of the Ejina Basin. a To the morphogenetic regions, b to the intensity of fluvial action, c to the type and the intensity of the predominant processes in a Peltier diagram. The base-graphs were after Peltier [42]

DOI: https://doi.org/10.30564/jgr.v2i1.1942

is weak, the chemical weathering is weak, the comprehensive weathering (physi-chemical weathering) is weak, the gravity transportation is weak, the aeolian action/wind-accumulation is strong, the proluvial action (flood erosion) is strong, the fluvial forces such as rivers, lakes and mudflows are moderate and partially weak, no glaciation action, the periglacial action is weak, the frozen-soil action is weak, the desiccation-denudation (wind erosion) action is strong (Figures 14-15).

Summarizing the analysis results of the Peltier model map (Figures 14-15) and considering the modern climatic conditions, the main geomorphoclimatic dynamics with relatively strong power and energy are the processes of desiccation-denudation (wind erosion), eolian/wind-accumulation, and flood erosion in the Ejina Basin. In addition, there is a process with weak to medium power in the Ejina Basin, i.e. the fluvial forces. Other common geomorphoclimatic processes, such as frost/freezing and chemical weathering, are weak. The processes those related to glaciers, periglaciers, and frozen soils have little or no effect in the basin. In brief, the main geomorphic dynamics in the Ejina Basin are wind force and water force.

3.3 Interaction of Aeolian and Fluvial Processes in the Ejina Basin

When the average temperature of the coldest month in a desert area is generally lower than 0 ° C, it can be defined as a cold desert environment (relative to the hot and temperate desert environment) [43]. The most remarkable characteristics of this desert environment are the existence of huge thermal interannual oscillations. According to this standard, the Ejina environment belongs to a cold desert environment, because the average landsurface temperature of the coldest month in winter since 1965-2005 varies from - 15 ° C to - 25 ° C in the basin.

Based on the rules of occurrence of the significant landsurface processes and the dominant geomorphic types in the cold desert environment, we can identify the geomorphic processes in specific areas. Generally, two most important geomorphic processes can be identified in desert environment [44], one is dominated by wind dynamics and the other is dominated by water dynamics. This can be seen from the dominant types of the climate-driven landforms in the Ejina Basin that the aerodynamic and waterdynamic landforms coexist on a wide spatiotemporal scale in the Ejina Basin, so the two geomorphic dynamics may be superimposed in the Ejina Basin. Sedimentary records in the Ejina Basin can also prove this, such as the sedimentary sequences interbedding of eolian and fluvial sediments in stratigraphic profiles (Figure 14) and sand dune deposited along the riparian zone of the Ejina River (Figure 9).

In geomorphology, typical aeolian landforms usually occur in areas with annual average precipitation less than 30 mm [38]. Dry climate promotes the development of mobile sand dunes, whereas these sand dunes become stable under humid conditions [38]. However, unlike the deserts in northern China, aeolian dunes in the Ejina Basin are mainly distributed on both sides of the river banks or nearby the river and the alluvial deposits, indicating that the formation of the aeolian landforms is largely affected by the fluvial or alluvial/proluvial process [33-34, 45]. A similar pattern of the sandy dune development was also observed in the Qaidam Basin [46]. The development of sand dunes along the Ejina River is abnormal because the river course and the surrounding areas are relatively humid but not dry. Regarding to the above-mentioned requirements for the formation of aeolian dunes in desert environment, as well as the fact that the landform in the central Ejina Basin is mainly Gobi landform with relatively flat terrain and consolidation of clastic sediments (that is to say, the process of wind erosion may be stronger than that of wind accumulation and the source of clastic material is deficient with sand sediment being not available) (Figure 6), the role of rivers on the development of sand dunes in the Ejina Basin may not inhibit the formation of aeolian dunes but provide the underlying uneven surface conditions and the potential source materials.

In the view of sedimentology, the riverbed surface sediments of the Ejina river is coarser downstream along the river channel [45], rather than finer downstream as other rivers in the world being [47-48]. Moreover, on the basin scale, the griansize of sand dune sediments in the Ejina Basin become finer gradually from south to north, which is consistent with the hydrological pattern of the basin, but not match to the composite direction of the prevailing wind system “from north to south” in the basin [33]. The sedimentological anomalies of fluvial and aeolian sediments on the spatial scale in the basin indicate an effective interaction and superposition effect of aeolian and hydraulic processes in shaping the basin landforms.

The above-mentioned geomorphological and sedimentological anomalies in the Ejina Basin indicate that the sediment supply of rivers and playas, the retation and blocking effect of river channels and related riverbank vegetation (such as Populus euphratica) on aeolian sediments, the relatively uneven underlaying surface conditions builted by river system and its weakening effect on local deflation process may be the key factors for the formation of sand dunes in the Ejina Basin, which may be even more important than the dry climate. In addition, the sedimentological changes of grain size of aeolian dunes

DOI: https://doi.org/10.30564/jgr.v2i1.1942

on the basin scale seem to be related to the local-scale factors such as hydrological processes in the Ejina Basin, but be decoupled with the regional-scale wind conditions. On the other hand, the temporary addition of aeolian sediments to the river sediments may be an important reason for the sedimentological anomaly of the downstream coarsening of river sediments along the Ejina River. It can be said that seasonal or transient rivers can be used as sediment interceptors to prevent the downwind movement of aeolian sediments. On the contrary, the aeolian sediment transportation can also affect the downstream distribution of river sediments. All of these indicate that there is a wide range of interaction between winddynamics and waterdynamics in the Ejina Basin.

It has been reported that in an arid environment, the interaction between aerodynamics and riverdynamics can occur at the dune unit scale, the desert landscape scale or the watershed scale [49]. Especially at dune unit scale, the interaction between aerodynamics and riverdynamics will affect the scope, shape and boundary of dunes field [50], as usual, the perennial river will directly restrict the downwind boundary of sand dunes development, while the temporary river will become the potential boundary of some sand seas. For example, the Orange River constrains the southwest boundary of dune downwind development in the southern Kalahari Desert in Africa [51], the Colorado River constrains the boundary of dune downwind development in the Algodones desert in Southern California of North America [52], and the dune range in northern Sudan of Africa ends on the Nile River [50]. The deserts bordered by temporary rivers are like the Wahiba Desert in North America, which ends at the intermittent wadi al batha River [53], and the Namib Desert in Central Africa, whose downwind desert edge ends at the kuiseb river [50].

Regarding to the contact relationship between different sedimentary stratigraphic sequence and the upper and lower layers, as well as field investigation and remote sensing images (Figures 2, 6, 16), the desert plain (Gobi), as a main geomorphic unit in the central Ejina Basin, was transformed from the landform of alluvial/proluvial fans, which had originated from the alluvial/proluvial process of the Ejina river. As mentioned above, desert plain is a landform that has experienced the relatively balanced geomorphological processes between the wind dynamics and the water dynamics [38], and the ideal annual mean precipitation for the formation of desert plain is 30-60 mm. From this standard of climate geomorphology, the current climate conditions of the Ejina Basin are suitable for the formation and development of desert plain. Therefore, the Gobi landform should be a modern geomorphic type in the Ejina Basin. However, from the remote sensing image (Figure 2), we can still recognize that there are large areas of alluvial fan landform in the basin, and there are also many residual landforms of riverbeds and river terraces. These mean that the Gobi landforms are still at the initial stage of its formation in the Ejina Basin.

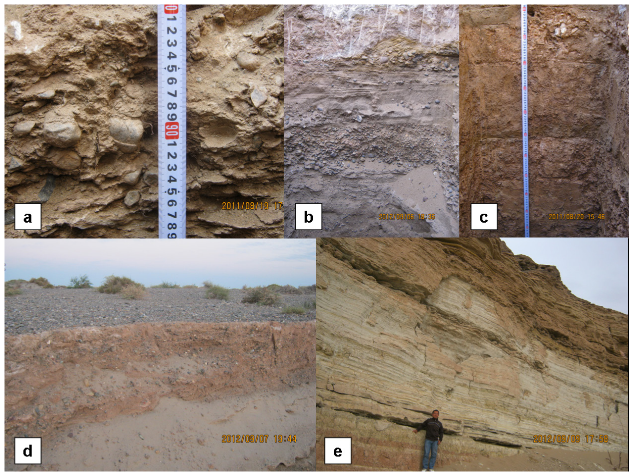

Figure 16. Sedimentary Profiles in the Ejina Basin: (a) proluvial-alluvial deposits (in desert plain), (b) complicated sedimentary sequence including sand, gravel, silt and clay sediments involved alluvial, fluvial, lacustrine and aeolian processes (in desert plain), (c) thick clayey deposits, (d) erosional terrace of river bank (margin of the basin), (e) palaeo-lacustrine section (at the low terrain of the north basin)

According to the contact relationship of stratigraphic layers, field observation and on-the-spot images, the formation of desert gorge landform is located at the upper part of the pediment and desert plain landforms in the Ejina Basin, and these gorge landforms often cut the mountain fronts (Figures 7, 8). Geomorphologically, the gorge and gully landforms are usually formed by the hydraulic process. Field investigation also confirmed this, because the signs of strong former erosion can be clearly observed on these landforms (Figure 8). In some places, loose sandy layers with unequal thickness have begun to cover the surface of these desert gorges. Geomorphologically, the formation of these sand layers should be aeolian origin and has experienced different degrees of desiccation-deflation processes due to drought conditions (Figure 8d). All these geomorphological evidences indicate that the aeolian and fluvial processes in the Ejina Basin are widely in progress.

3.4 Palaeo-environmental Indications of Landforms in the Ejina Basin

To understand the formation and evolution of landforms at different spatiotempotal scales in arid environment, on the one hand, it is necessary to identify the geomorphic

DOI: https://doi.org/10.30564/jgr.v2i1.1942

types and related morphogenetic and morphodynamic mechanisms, on the other hand, it is also dependent on whether good chronological data controlling the involved sedimentary events can be obtained for these landforms [49]. Based on the climatic implications of different modern landforms and deposits, one can also estimate the past climate changes indicated by ancient landforms and deposits [54], that is, to adopt the principle and method of "historical comparison" (namely that the present is the key to the past). For example, Hoevermann [39] calculated the annual mean precipitation of the Qaidam Basin in the past 32 Ka, by comparing the annual sedimentation rate of clastic sediments in core CK 2022 from the central Qaidam Basin with that of modern lakes. Also, Goudie [55] suggests that the area with the global largest frequency of duststorm at present or in the past is located in the area with rainfall between 100-200 mm/a, which is consistent with many modern observations from regions of Tibet, Mongolia and Africa [38, 56-58].

3.4.1 Environmental Indications of Relict Landforms in the Ejina Basin

The climate prerequisite for the formation of a peneplain (pediment) landform is a cold winter and an annual mean precipitation of 150-300 mm [38]. Of the great important for its morphogenetic mechanism is that the frost weathering in winter and the fluvial/alluvial/proluvial processes in summer are alighed with the formation of pediment. However, the current annual mean precipitation and temperature in the Ejina Basin are only 35 mm and 8.8 ℃, respectively (Figure 4). Under the current climatic conditions, the process of desiccation-denudation (dry erosion) has dominated the whole year and only weak to moderate fluvial/alluvial/proluvial processes exist in the sasin [34]. Therefore, the current climatic and environmental conditions in the Ejina Basin can not form a real pediment landform.

The formation of the desert gorge landform in the Ejina Basin requires a strong erosion process of flowing water. The critical annual precipitation for the development of desert gorge landforms is considered to be 60-150 mm [38]. But at present, the ground surface of these gorge landforms in the Ejina Basin is usually bare, and the current process of frost weathering is also weak due to lack of water. Therefore, similar to the pediment landform, the current Ejina Basin cannot form a true desert gorge landform due to water shortage.

According to Hoevermann [38], whether it is desert gorge or pediment landform, the formation of both the two landforms reflects the existence of a climate that has more annual average precipitation and lower temperature than the current. Therefore, the pediment and desert gorge landforms in the Ejina Basin are residual landforms (i.e. ancient landforms) related to the humid and cold climate in the past. At present, due to the prevalence of aerodynamic process and the existence of temporary fluvial/alluvial/proluvial processes, the pediment and desert gorge landforms are transforming into desert plains [34]. In addition, the widespread occurrence of mobile sandy dunes and the presence of large-scale ancient lake beds indicate that the current drought index of the Ejina Basin is increasing [34].

Landforms such as pediment and desert gorge in the Ejina Basin are also widely distributed in the northern, eastern and southern parts of the Alashan Plateau (Figures 2, 17) and in the desert regions in western China (Figure 1, [34]). In view of the climatic geomorphology, the extreme arid and mid-latitude temperate climate backgrounds of the western China and the Alashan Plateau as a whole currently indicate that these landforms are residual landforms and are related to a humid and cold climate in the past. Geochronological studies from the lacustrine sedimentary sections in the central Alashan Plateau [39-40] indicate that the Alashan Plateau was in a humid and cold climate during the local glacial maximum of the last glacial period, which is consistent with the environmental conditions required for the formation of pediment and desert gorges around the plateau. Field investigations show that the desert regions of western China have experienced obvious climate fluctuations in the Late Quaternary, accompanied by clear changes in landforms and paleohydrological environments [7,18-19,54,59-66]. Sand dunes and desert plain landforms are currently being formed in these areas, but the underlying residual landforms of desert gorges and alluvial fans should have been formed during the local glacial period [6,40]. Regarding to the comparability in geomorphology and sedimentology between different areas with similar hydroclimate (both arid areas), especially these areas have a similar low degree of weathering [67], it may be logically reasonable to attribute the development age of the residual landforms such as desert gorges and pediments around marginal areas of the Ejina Basin to the local glacial maximum of the last glaciation. This idea is also supported by many sedimentary chronological data of similar arid areas. For example, studies have shown that during some glacial ages (approximately 32-24 ka) in Central Asia, northern China, Mongolia, and the Qinhai-Tibetan Plateau, the climate in these areas was more humid and cold [2,5-6,10,68]. Widely distributed residual ice wedges and moraine deposits in the Qaidam Basin and Tarim Basin of northwestern China indicate that the coldest period of the last glaciation in the two basins is about 30-25 ka. Sequential sandy-dune sediments and high palaeo-lake levels in the Badanjilin Desert and its adjacent areas (such as Mongolia) indicate that the climate of north-central China and Mongolia during the marine oxygen isotope stage-three (MIS3) is much more humid than it is today [6]. The Loess Plateau of western China also had a cold and wet climate during MIS4 and MIS3 [5]. The north boundary of the Great Gobi in Mongolian has shrunk by nine times due to the humid climate in different periods of the past 40 ka, such as about 34.4ka, 30.7ka, 28.9ka, 24.5ka and 15.09 [71].

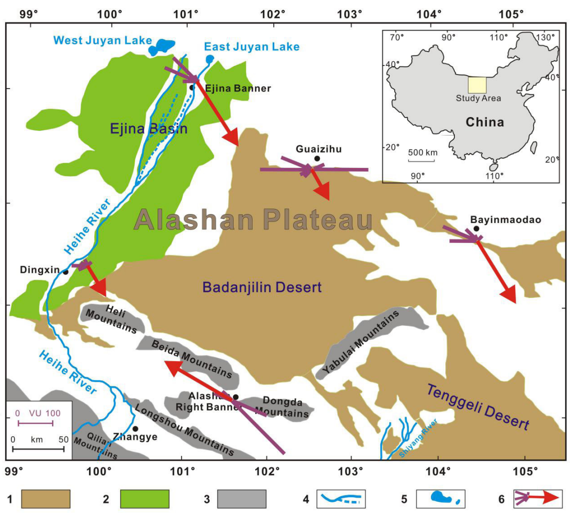

Figure 17. Landscapes of the Alashan Plateau (modified from Yang et al. 2011b). The compound directions of wind systems in different areas in the Alashan Plateau are also shown in the panel

Note: Legend 1 sand dunes, 2 fluvial/alluvial sediments associated with the Heihe River, 3 adjacent mountain ranges, 4 rivers, 5 lakes, and 6 sand roses (Fryberger and Dean 1979) for five surrounding weathering stations, with purple lines showing winds capable of transporting sand from various directions (DP, vector units with wind speed in knots VU) and red lines with arrows indicating the resultant sand transport trend (RDP, vector units in VU)

It has been reported that the marginal and central areas of the Alashan Plateau experienced a wide range of pedimentation processes during the last glacial period [39]. Researchers also identified three different stages of formation of pediment landforms at the foreland of the Qilian Mountains during the Pleistocene [39]. In view of the climatic geomorphology, the annual mean precipitation of these regions should be as high as 150-300 mm during the development of pediment landform. However, the current multi-year climate records from meteorological stations show that the annual mean precipitation in the southeast of the Alashan Plateau is only 110 mm, in the northwest is only 38 mm, and in the Ejina Basin is only about 36.5 mm (Figure 4a). Comparing the current climate of the Alashan Plateau with the corresponding climatic conditions when the desert gorge landform (60-150 mm) and the pediment landform (150-350 mm) were formed, then the variation range of precipitation during the last glacial period in the Alashan Plateau should be at least 20-200 mm, which is much larger than the modern climate level; while the annual mean precipitation in the marginal areas of the Ejina Basin is about 60-350 mm during the LGM period, an increase of 50%-775 % than that today.

3.4.2 Environmental indications of modern landforms in the Ejina Basin

As mentioned above, the geomorphic types of desert plains (Gobi) and aeolian sandy dunes represent the landforms of modern orgin in the Ejina Basin, because the current climate of the Ejina Basin match the environenntal conditions for their formation and development in view of the climatic geomorphology. Under arid condition, the Gobi landform transformed from alluvial fans is a common phenomenon [69]. Evidences from stratigraphic profiles of remotely sensed images reveal that the Gobi landform in the Ejina Basin has also been extensively transformed from the original alluvial deposits (Figures 6, 16). Due to the reason that the formation of the Gobi landform requires a morphodynamic balance between aeolian and hydraulic processes, while the balance between these two dynamic factors cannot be simply explained by climate change in an arid environment because the results of climate change on the two agents are usually opposite, thus the adjustment and influence of tectonic activities must be considered. Therefore, reconstructing the evolutionary history of the Gobi landform is of great significance for revealing regional-scale tectonic activities and climate changes [5, 70-71]. In addition, the formation and evolution of alluvial fan are also closely related to regional tectonic activities and climate change [35]. In climatic geomorphology, sudden floods and strong winds are the two main driving factors for the formation of Gobi desert [35, 38]. As a result, the Gobi sediments expericed the processes of hydraulic transport and wind erosion and the related changes in tectonic acvtivities and climate are also recorded. In genetics, the beginning of the development of a Gobi landform represents the end of the evolution of an alluvial fan [35].

The content of cosmogenic nuclide ^{10}Be in the quartz gravel sediments on the Gobi surface in the Ejina Basin has been systematically measured [72-73] to evaluate the exposure age of these Gobi gravels. The results show that the exposed ages of the Gobi gravels in the northern edge of the Ejina Basin are more than 420 Ka, while those of the "Central Gobi" gravels in the Ejina Basin are 190 Ka (Figure 18). Judging from the spatial and temporal chang-

  DOI: https://doi.org/10.30564/jgr.v2i1.1942

es of the ^{10}Be ages, the gravels in the Central Gobi gradually developed northward and eastward until the modern lake area at the end of the Ejina River. The spatiotemporal variation of the ages of the Gobi gravel outcrops in the Ejina Basin indicates that they are the result of the alluvial process influenced by the uplift and tectonic activities of the Qinghai-Tibet Plateau [73]. The 10Be ages of the cosmic origin of the Gobi gravels indicate that the end of alluvial process and the beginning of the formation of Gobi landform in the northern edge of the Ejina Basin occurred before 420 Ka, while the formation of the Central Gobi in the Ejina Basin occurred before 190 Ka (Figure 18). The two critical periods are both in the glaciation ages of late Pleistocene.

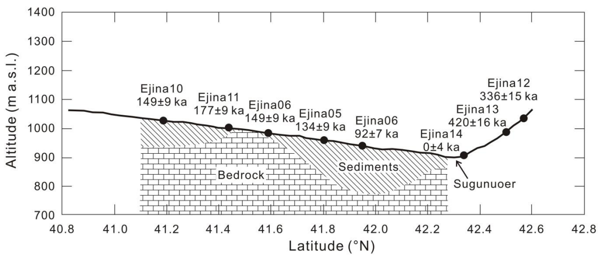

Figure 18. Variations in altitude, sediment thichness, and exposure ages of the quartz gravels from the Gobi deserts along a SW-NE transaction in the Ejina Basin (after Zhang et al., [72] and Lv et al., [73])

The episodic formation of Gobi desert in the past 420 Ka indicates that the advance and retreat of alpine glaciers in glacial / interglacial cycles may be the main factors affecting the intensity of alluvial process and river water discharge in the Ejina Basin [72-73]. However, the strong proluvial (flooding) process and large amount of water could mainly occur in the short disglacial ages.

Since the formation and development of landforms between the Gobi and the alluvial fan have an inherited relationship in time, the source of sediments in the Gobi landform of the Ejina Basin may be closely related to ancient alluvial deposits, but not to modern river sediments. The differences in grain size sedimentology between the Gobi sediments in the Ejina Basin and the riverbed sediments from the Ejina Basin also show this point [45].

For arid intermountain basins in Cetrnal Asia, a large number of clastic sediments derived from alpine river transportation are stored in alluvial fan landform or become basin fillings [1-2]. The depositional process of alluvium is related to the land surface instability caused by regional climate change [35, 69]. It is worth noting that one of the landform characteristics of the Ejina Basin is its geomorphological instability under current climatic conditions [34]. For example, geomorphologically, the ancient alluvial fan landform in the Ejina Basin is changing to desert plain landform, which can be proved by remote sensing images, the changes of sedimentary facies in the Gobi stratigraphic profiles, and the huge thickness of alluvial/proluvial strata widely distributed on the profiles (Figures 2, 16).

From the geomorphological perspective of the entire Central Asia, ancient alluvial fan landforms can be divided into two basic types: the decomposed alluvial fan and the undecomposed alluvial fan [74]. Most of the decomposed alluvial fans consist of relatively older surfaces (early to middle Pleistocene), while most of the undamaged alluvial fans have younger surfaces (late Pleistocene to Holocene) [74]. The distribution of alluvial fans formed in the Middle Pleistocene or earlier is relatively limited. Due to the relative uplift of the fan toes, the well preserved ancient alluvial fans are only limited to the area where the fan surface inclines rapidly toward the fan tip [75]. The alluvial fans at the southern margins of the Tarim Basin in Western China are typical examples of this type [74]. In the Ejina Basin, however, the ancient alluvial fan buried in the desert Gobi landform has hardly been destroyed. Through comparative analysis with the Tarim Basin, it can be considered that the alluvial fan landform of the Ejina Basin is younger than that of the Tarim Basin, and the alluvial fans in the Ejina Basin should have developed since the late Pleistocene. This is consistent with the ^{10}Be exposure ages of the Gobi gravels mentioned above.

3.4.3 Environmental Indications of Chronological Records in the Ejina Basin

Over the past decades, great progress has been made in geochronology of the Ejina Basin and the Aashan Plateau. For example, many studies have conducted geomorphological and chronological surveys on the three ancient lake basins in the Ejina Basin (Gashunuoer Lake Basin, Sugunuoer Lake Basin and Juyanze Basin). Evidences from studies of ancient lake shorelines and sedimentary cores of these lake basins indicate that these areas experienced severe environmental changes during the Holocene [76-78]. Almost all of these studies show that the climate fluctuated greatly during the Holocene in the Ejina Basin and in the Alashan Plateau [11, 79-84], which is related to the dynamic changes of the Asian monsoon or/and the westerly circulation flowing through China that follows the changing trend of the insolation patterns of northern hemisphere [10, 80].

The ancient river bed and ancient lake bed landforms in the Ejina Basin are numerous and can be identified from field observations or remotely sensed images (Figures 2, 13, 16). According to field investigations and the geomorphological mapping of the water level of the Sugunor Lake, we calculated that the high lakewater level of the

DOI: https://doi.org/10.30564/jgr.v2i1.1942

ancient Sugunor Lake was nearly 40 m above the current lakewater level. Investigations in the area of Guaizi Lake in the northern Badanjilin Desert show that there are three levels of high terraces on the south bank of the lake, and the highest terrace is about 40 meters higher than the modern lake bed. A survey at the Guinai Lake revealed that the ancient lake terrace in the southern part of the lake basin was more than 20 meters above the modern river bed. In previous studies, the height of lake bed of the Gashunor Lake is regarded as zero base level, then the highest terraces around the Sugunor Lake and the Juyanze Lake are 34 m and 33.6 m higher than the bed of Gashunor Lake, respectively [85]. Since there is no bedrock mountain range between the Gashunor and sugunor lake basins, and there are lower terrain channels connecting the Juyanze lake basin and Sugunor lake basin, it can be reasonably assumed that in the past period with high lake levels, the water surfaces of the three lakes were connected together to form a whole. The radiocarbon age of the shell samples collected from the uppermost terrace of the Sugunor lake Basin showed that the sedimentary age was about about 33.7 Ka during the last glaciation [85].

Studies have reparted the results of geochronological analysis of sedimentary cores from the Gashunor and Sugunor lakes in the Ejina Basin [76]. The geochronology data of these lakes are from 62 ^{14}C dating results. In the areas of the Gashunorake and Sugunor lakes, the geological ages of the sedimentary terraces with the highest lakewater levels, which are about 28m to 32m above the modern lake bed, occur between 14 ka and 33 ka. The water levels of the Gashunnuo Lake dropped by about 15 meters and 18 meters at about 21 ka and 19 ka, respectively. After 19 ka, the areas of the Gashunnuor and Sugunuoer lakes were arid, and the sand dune sediments continued to be deposited until 14 ka. In addition, no dating data and materials were available between 18.6 Ka and 12.8 Ka. This phenomenon supports the state of aridity during this period, because the lacustrine sedimentation process in an arid environment will lack organic matter and thus radiocarbon dating materials, resulting in the discontinuous chronological data. After 11.3 ka, a freshwater lake appeared in the areas of the Gashunor and Sugunor lakes.

The ancient Juyanze Lake in the eastern Ejina Basin (Figure 13d) (41.75-42°N, 101.5-102°E) provides evidence of the complex hydrological pattern in the area in the Holocene [86]. The lithology, geochemistry and mineralogy data of the lake's sedimentary core show that there are significant differences between the lakes in the early, middle and late Holocene. During the period of about 10,700 cal BP, the lake began to become a fresh water lake, formed in the regional extreme runoff events affected by humid climate. During the period of about 8900 to 8100 cal BP, the runoff in this lake area was very small. Compared with the humid climate in the early Holocene, the rainfall conditions from the middle to late Holocene are not obvious, and it shows a general trend of drying up completely of the lake [86].

3.5 The Conceptual Model Coupling Landform and Climate

Over the years, geomorphologists and paleoclimatologists have summarized the different geomorphological processes and different paleoclimatte evidences in the basins and mountain areas in Central Asia since the late Quaternary (the past 100000 years) [6,54,58,63,87-88]. The relationship between these landforms and environmental changes is summarized into a conceptual model. The schematic diagram of the model is roughly shown in Figure 19. Among them, the climate fluctuations of glaciations are based on the research results of glaciers on the Tibetan Plateau [2,54,87]. In the Qinghai Tibet Plateau and the surrounding mountainous areas, the expansion of the largest glaciers occurred during two stages of the last glaciation (i.e. MIS4 and MIS2 at about 70-50 Ka and 32-14 Ka, respectively, particularlly the late glaciation at about 15 ka), and the expansions of these glaciers have promoted the development of desert gorge and pediment landforms in these areas [87-87]. While during MIS 3, these areas were in a relatively humid climate because of the high water levels in some lakes. Overall, the establishment of this conceptual model, which couples the landforms and climatic environment in Central Asia since the late Pleistocene, provides an important clue for understanding the relationship between landforms development and climate fluctuations in the Ejina Basin since the last glacial period under a large-scale background.

The wide distribution of the Gobi desert landforms in Central Asia is mainly derived from alluvial fan landforms and pediment landform with fanglomerates accumulation. As shown in Figure 19, there is a transition from humid (mainly MIS3) to arid climate in most parts of Central Asia. The observation of Late Quaternary alluvial fans in the Gobi deserts, southern Mongolia, indicates that there may be more humid conditions between 40-23 Ka, followed by a dryer period [63]. The highest water level (28-32 m) in the past occurred between 41 and 33 ka in the Gashunnuoer-Sugunuorhu lake area of the Ejina Basin [76,85]. Compared with the climate of the Ejina Basin today, the appearance of these high lake water levels should be related to the high palaeo-precipitation and palaeo-hydrological cycle in the past.

DOI: https://doi.org/10.30564/jgr.v2i1.1942

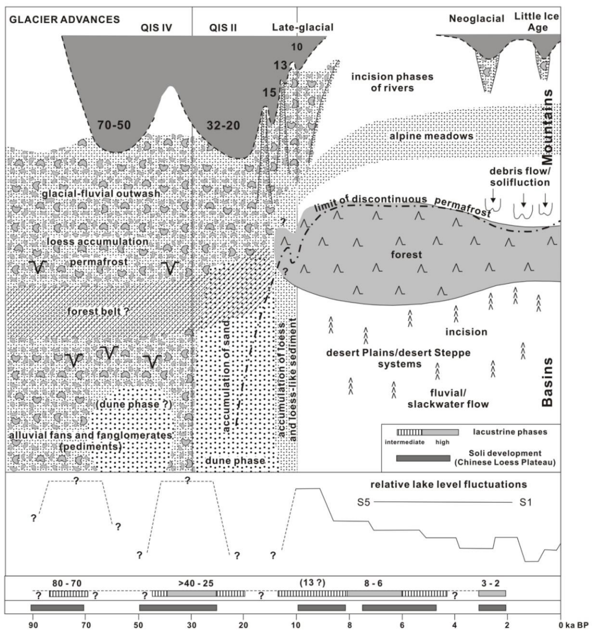

Figure 19. A conceptal model of Landform and climate in central Asia including lake level changes, glacier fluctuations in the mountains (top) and basins (bottom) of northern China and Mongolia during the late Pleistocene (Modified from [54,88])

In terms of climate genesis, the increase of precipitation in western Inner Mongolia (including the Alashan Plateau and the Ejina Basin) during the last glacial period may be due to the enhanced westerly circulation [6]. Benn and Owen [87] also suggested that glaciers in the northern Tibetan Plateau and northern Karakoram also responded to changes in the westerly circulation during the late Pleistocene. The humid climate in western Inner Mongolia during the Anaglacial period (about 32-24 ka) may be caused by the enhancement of the Westerly circulation and the weakening of the Winter Monsoon Circulation [54]. The changes of the two circulation systems both influence the western region of Central Asia first, while the latter (winter monsoon) affects mainland China and eastern Central Asia. The drought in western Inner Mongolia during the Kataglacial period (approximately 24-15 ka) may be due to the great movement of the Siberian High to the south and the strengthening of the Winter Monsoon, which led to arid climate in northern and central China [90-92]. Therefore, the different climate changes during the glacial period in western Inner Mongolia, especially the changes in precipitation, may be mainly affected by changes in the Siberian high-pressure system and its thermal effects. The persistent enhancement of the Siberian high in winter and spring may significantly increase the gradients of the wind and temperature fields in the surrounding area; while the relatively weak and northward contraction of Siberian high system will increase the cyclonic precipitation brought by Westerly circulation or/and monsoon circulation in spring, resulting in the humid climate in Central Asia.

The high lake level is evidence of a relatively humid climate in the early Holocene in the central Alashan Plateau [6, 40]. However, the pollen data records of the core of Lake Sugunor in the Ejina Basin did not show that the area was the wettest in the early Holocene [93]. The results of these studies indicate that the water supply in the arid area of Inner Mongolia during the Holocene period may be very unstable or has obvious regional differeces. Because the East Asian Summer Monsoon circulation interacts with the Westerly circulation at the northern boundary of the summer monsoon, variations between dry and wet climate conditions in western Inner Mongolia may be more pronounced than other regions in China controlled by monsoon climate.

4. Conclusion

The formation of landforms on earth mainly depends on internal and external forces. The internal force, especially the tectonic movements since the Mesozoic and Cenozoic, are the overall constraints of the current mountain-basin coupling landforms in the Ejina Basin and even the Alashan Plateau. The external force is mainly controlled by climatic factors, which is the main reason for the geomorphodiversity of the Ejina Basin. Desert plain (Gobi), pediment, desert gorge, aeolian dune, fluvial channel and ancient lacustrine plain are the main existing geomorphic units in the basin. This study shows that there is a close relationship between the geomorphoclimatic processes and the landforms in the Ejina Basin. From the perspective of climate geomorphology, the existence of peneplain (pediment) landform shows that the study area has experienced high precipitation and frost/freezing and weathering process, that is, there was a humid and cold climate. The landform of desert gorges on the edge of the basin is an ancient landform eroded by running water or melting water. Flood erosion and wind action are the main geomorphic dynamics in the basin under the present climate. They are also the main geomorphodynamics for the formation of the Gobi desert landform. Aerodynamic and Gobi landforms usually occur in areas where the annual mean precipitation is less than 30-60 mm. Small sandy dunes are widely distributed along the Ejina River, and the Gobi desert landform is the main geomorphic type in the central basin. At present, the average annual precipitation in the Ejina Basin is about 35mm, indicating that the landforms of desert plain and aeolian dune are contemporary landforms that match the current climate. The existence of ancient landforms such as pediment and desert gorge

 DOI: https://doi.org/10.30564/jgr.v2i1.1942

indicates that the range of precipitation variation in the past has reached 20 to 200 mm, which is much greater than the current climate level. The coexistence of these ancient landforms and contemporary landforms shows that the diversity of basin landforms is the result of the joint effect of tectonic activities, freeze-thaw and weathering, fluvial, alluvial/proluvial and aeolian processes, as well as climate change. Previous evidences have proved that the geomorphology of Central Asia is mainly the result of Quaternary climate change, which has forced changes in the environment of piedmont regions and basins. The landform evolution of the Ejina Basin further confirmed this, and the geomorphological evolution of the Ejina Basin since the late Pleistocene has been greatly influenced by external forces (climate). The study of the ancient lake geomorphology and sedimentation in the lowest marginal area of the basin shows that the arid environment in the region has changed drastically since the last glacial period. It experienced a humid climate and high precipitation at 39-23 ka BP and obvious climate fluctuations during the Holocene. Due to the relatively weak Asian summer monsoon in the glacial period, the changes in the Westerly circulation during the late Pleistocene and the regulation of the Siberian high system may be the main factors affecting the climate change in the Ejina Basin and in the trtire Alashan Plateau.

Acknowledgments

The study was financially supported by the National Natural Science Foundation of China (grant nos. 41930640, 41771014) and the Project of the Second Comprehensive Scientific Investigation on the Qinghai Tibet Plateau (2019QZKK1003). Sincere thanks are extended to Profs. Xiaoping Yang, Bernd Wünnemann, and Frank Lehmkuhl for their generous help in the study work.

References

[1] Liu, T., Ding, M., Derbyshire, E.. Gravel deposits on the margins of the Qinghai-Xizang Plateau, and their environmental significance. Palaeogeography Palaeoclimatology Palaeoecology, 1996, 120: 159-170.

[2] Liu, T., Zhang, X., Xiong, S., Qin, X., Yang, X.. Glacial environments on the Tibetan Plateau and global cooling. Quaternary International, 2002, 97-98: 133-139.

[3] Liu, T., Ding, Z.. Chinese loess and the paleomonsoon. Annual Review of Earth and Planetary Sciences, 1998, 26: 111-145.

[4] Sun, J., Ding, Z., Liu, T.. Desert distributions during the glacial maximum and climatic optimum: example of China. Episodes, 1998, 21: 28-31.

[5] Feng, Z., Chen, F., Tang, L., Kang, J.C.. East Asian monsoon climates and Gobi dynamics in marine isotope stages 4 and 3. Catena, 1998, 33: 29-46.

[6] Yang, X., Rost, K.T., Lehmkuhl, F., Zhu, Z., Dodson, J.. The evolution of dry lands in northern China and in the Republic of Mongolia since the Last Glacial Maximum. Quaternary International, 2004, 118-119: 69-85.

[7] Yang, X., Scuderi, L. A., Paillou, P., Liu, Z., Li, H., Ren, X.. Quaternary environmental changes in the drylands of China: a critical review. Quaternary Science Reviews, 2011, 30: 3219-3233.

[8] Yang, X., Li, H., Conacher, A.. Large-scale controls on the development of sand seas in northern China. Quaternary International, 2012, 250, 74-83.

[9] Ding, Y., Chan, J.C.L.. The East Asian summer monsoon: an overview", Meteorology and Atmospheric Physics, 2005, 89: 117-142.

[10] Herzschuh, U.. Palaeo-moisture evolution in monsoonal Central Asia during the last 50,000 years. Quateranry Science Reviews, 2006, 25: 163-178.

[11] Wunnemann, B., Hartmann, K., Janssen, M., Zhang, H.C.. Responses of Chinese desert lakes to climate instability during the past 45,000 years. Developments in Quaternary Science, 2007, 9: 11-24.

[12] Stevens, T., Lu, H., Thomas, D.S.G., Armitage, S.J.. Optical dating of abrupt shifts in the Late Pleistocene East Asian monsoon. Geology, 2008, 36: 415-418.

[13] Yang, S.L., Ding, Z.L.. Advance-retreat history of the East-Asian summer monsoon rainfall belt over northern China during the last two glacialeinterglacial cycles. Earth and Planetary Science Letters, 2008, 274: 499-510.

[14] Yang, S.L., Ding, Z.L., Li, Y.Y., Wang, X., Jiang, W.Y., Huang, X.F.. Warming-induced northwestward migration of the East Asian monsoon rain belt from the Last Glacial Maximum to the mid-Holocene. Proceedings of the National Academy of Sciences of the United States of America, 2015, 112: 13178-13183.

[15] Mason, J.A., Lu, H., Zhou, X., Miao, X., Swinehart, J.B., Liu, Z., Goble, R.J., Yi, S.. Dune mobility and aridity at the desert margin of northern China at a time of peak monsoon strength. Geology, 2009, 37: 947-950.

[16] Lu, H., Mason, J. A., Stevens, T., Zhou, Y., Yi, S., Miao, X.. Response of surface processes to climatic change in the dunefields and Loess Plateau of North China during the late Quaternary. Earth Surface Processes and Landforms, 2011, 36: 1590-1603.

[17] Li, Q., Wu, H., Yu, Y., Sun, A., Markovic, S. B., Guo, Z.. Reconstructed moisture evolution of the deserts in northern China since the Last Glacial Maximum and its implications for the East Asian Summer Monsoon.

  DOI: https://doi.org/10.30564/jgr.v2i1.1942

Global and Planetary Change, 2014, 121: 101-112.
[18] Yang, X., Scuderi, L.A.. Hydrological and climatic changes in deserts of China since the late Pleistocene. Quaternary Research, 2010, 73: 1-9.
[19] Yang, X., Scuderi, L., Liu, T., Paillou, P., Li, H., Dong, J., Zhu, B., Jiang, W., Jochems, A., Weissmann, G.. Formation of the highest sand dunes on Earth", Geomorphology, 2011, 135: 108-116.
[20] Yang, X., Wang, X., Liu, Z., Li, H., Ren, X., Zhang, D., Ma, Z., Rioual, P., Jin X., Scuderi, L.. Initiation and variation of the dune fields in semi-arid northern China - with a special reference to the Hunshandake Sandy Land, Inner Mongolia. Quaternary Science Reviews, 2013, 78: 369 - 380.
[21] Scuderi, L., Weissmann, G., Kindilien, P., Yang, X.. Evaluating the potential of database technology for documenting environmental change in China's deserts. Catena, 2015, 134: 87-97.
[22] Guo, Z.T., Ruddiman, W.F., Hao, Q.Z., Wu, H.B., Qiao, Y.S., Zhu, R.X., Peng, S.Z., Wei, J.J., Yuan, B.Y. and Liu, T.S.. Onset of Asian desertification by 22 Myr ago inferred from loess deposits in China. Nature, 2002, 416: 159-163.
[23] Sun, J.. Provenance of loess material and formation of loess deposits on the Chinese Loess Plateau. Earth and Planetary Science Letters, 2002, 203: 845-859.
[24] Panizza, M.. The geomorphodiversity of the Dolomites (Italy): a key of geoheritage assessment. Geoheritage, 2009, 1: 33-42.
[25] Testa, B., Aldighieri, B., Bertini, A., Blendinger, W., Caielli, G., de Franco, R., Giordano, D., Kustatscher, E.. Geomorphodiversity of the San Lucano Valley (Belluno Dolomites, Italy): a well-preserved heritage. Geoheritage, 2013, 5: 151-172.
[26] Gordon, J.E., Barron, H.F., Hansom, J.D., Thomas, M.F.. Engaging with geodiversitydwhy it matters. Proceedings of the Geologists' Association, 2012, 123: 1-6.
[27] Beggs, P.J.. New directions: climatediversity: a new paradigm for climate science", Atmospheric Environment, 2013, 68: 112-113.
[28] Wang, X., Hua, T., Zhang, C.. Aeolian salts in Gobi deserts of the western region of Inner Mongolia: Gone with the dust aerosols. Atmospheric Research, 2012, 118: 1-9.
[29] Natsagdorj, L., Jugder, D., Chung, Y.S.. Analysis of dust storms observed in Mongolia during 1937-1999. Atmospheric Environment, 2003, 37: 1401-1411.
[30] Wang, X., Zhou, Z., Dong, Z.. Control of dust emissions by geomorphic conditions, wind environments and land use in northern China: An examination based on dust storm frequency from 1960 to 2003. Geomorphology, 2006, 29: 292-308.
[31] Wang, X., Xia, D., Wang, T.. Dust sources in arid and semiarid China and southern Mongolia: Impacts of geomorphologic setting and surface materials", Geomorphology, 2008, 97: 583-600.
[32] Liu Z.J., Tapponnier, P., Gaudemer, Y., Ding, L.. Quantifying landscape differences across the Tibetan plateau: implications for topographic relief evolution. Journal of Geophysical Research, 2008, 113: F04018. DOI: 10.1029/2007JF000897
[33] Zhu, B., Yu, J., Rioual, P., Ren, X.. Particle size variation of aeolian dune deposits in the lower reaches of the Heihe River basin, China. Sedimentary Geology, 2014, 301: 54-69.
[34] Zhu, B., Yu, J., Rioual, P., Gao Y., Zhang, Y., Min, L.. Geomorphoclimatic characteristics and landform information in the Ejina Basin, Northwest China. Environmental Earth Sciences, 2015, 73: 7547-7560.
[35] Gutierrez, M.. Climatic Geomorphology. Amsterdam, Elsevier, 2005.
[36] Mabbutt, J.A.. Desert Landforms", Cambridge, MA, The MIT Press, 1977.
[37] Guo, H., Liu, H., Wang, X., Shao, Y., Sun, Y.. Subsurface old drainage detection and paleoenvironment analysis using spaceborne radar images in Alxa Plateau. Science in China Series D, 1977, 43: 439-448.
[38] Hoevermann, J.. Das System der klimatischen Geomorphologie auf landschaftskundlicher Grundlage. Zeitschrift fur Geomorphologie Neue Folge, 1985, 56 (Supplementary Band): 143-153.
[39] Hoevermann, J., Hoevermann, E., Lehmkuhl, F. Geomorphologische Untersuchungen im noerdlichen Vorland des Qilian Shan, China. Berliner geographische Abhandlungen, 1998, 63: 83-98.
[40] Yang, X.. Late Quaternary evolution and paleoclimates, western Alashan Plateau, Inner Mongolia, China. Zeitschrift fur Geomorphologie Neue Folge, 2001, 45: 1-16.
[41] Mensching, H.G.. Inselberge, Pedimente und Rumpfflaechen im Sudan (Repubhk) - Ein Beitrag zur morphogenetischen Sequenz in den arid Subtropen und Tropen Afrikas. Zeitschrift fuer Geomorphologie, 1978, 30 (Supplementband): 1.
[42] Peltier, L.C.. The geographic cycle in periglacial regions as it is related to climatic geomorphology. Annals of the Association of American Geographers, 1950, 40: 214-236.
[43] Meigs, P.. The world distribution of arid and semiarid homoclimates. Riviews of Research on Arid Zone Hydrology, Paris, UNESCO, 1953: 203-209.
[44] Cooke, R.U., Warren, A., Goudie, A.. Deserts Geomorphology. London, UCL Press, 1993.

 DOI: https://doi.org/10.30564/jgr.v2i1.1942

[45] Zhu, B., Yu, J.. Aeolian sorting processes in the Ejina desert basin (China) and their response to depositional environment. Aeolian Research, 2014, 12: 111-120.
[46] Yu, L., Lai, Z., An, P., Pan, T., Chang, Q.. Aeolian sediments evolution controlled by fluvial processes, climate change and human activities since LGM in the Qaidam Basin, Qinghai-Tibetan Plateau. Quaternary International, 2015, 372: 23-32.
[47] Ferguson, R., Hoey, T., Wathern, S., Werritty, A.. Field evidence for rapid downstream fining of river gravels through selective transport. Geology, 1996, 24: 179-182.
[48] Frings, R.M.. Downstream fining in large sand-bed rivers. Earth-Science Reviews, 2008, 87: 39-60.
[49] Tooth, S.. Arid geomorphology: investigating past, present and future changes. Progress in Physical Geography, 2007, 31: 319-335.
[50] Bullard, J.E., Mctainsh, G.H.. Aeolian-fluvial interactions in dryland environments: examples, concepts and Australia case study. Progress in Physical Geography, 2003, 27: 471-501.
[51] Thomas, D.S.G., Stokes, S., Shaw, P.A.. Holocene aeolian activity in the southwestern Kalahari Desert, southern Africa: significance and relationships to late-Pleistocene dunebuilding events. The Holocene, 1997, 7: 273-81.
[52] Sweet, M.L., Nielson, J., Havholm, K., Farrelley, J.. Algodones dunefield of southern Caifornia: a case history of a migrating modern dunefield. Sedimentology, 1988, 35: 939-52.
[53] Warren, A.. The dunes of the Wahiba Sands. Special Report 3: the Scientific Results of the Royal Geographical Society's Oman Wahiba Sands Project 1985-1987. Journal of Oman Studies Special Report, 1988, 3: 131-60.
[54] Lehmkuhl, F., Haselein, F.. Quaternary paleoenvironmental change on the Tibetan Plateau and adjacent areas (Western China and Western Mongolia). Quaternary International, 2000, 65/66: 121-145.
[55] Goudie, A. S.. Dust storms in space and time. Progress in Physical Geography, 1983, 7: 503-530.
[56] Hoevermann, J.. Morphogenetic regions in Northeast Xizang (Tibet). In, Hovermann, J., Wang, W. (Eds.). Reports of the Qinghai-Xizang (Tibet) Plateau. Beijing, Science Press, 1987: 112-139.
[57] Hoevermann, J., Lehmkuhl, F., Portge, K.H.. Pleistocene glaciations in eastern and central Tibet - Preliminary results of Chinese-German joint expeditions. Zeitschrift fur Geomorphologie Neue Folge, 1993, 92 (Supplementary Band): 85-96.
[58] Lehmkuhl, F.. The spatial distribution of loess and loess-like sediments in the mountain areas of Central and High Asia. Zeitschrift fur Geomorphologie Neue Folge, 1997, 111 (Supplementary Band): 97-116.
[59] Chen, K., Bowler, J.. Late Pleistocene evolution of salt lakes in the Qaidam Basin, Qinhai Province China. Palaeogeography Palaeoclimatology Palaeoecology, 1986, 54: 87-104.
[60] Thompson, L.G., Mosley-Thompson, E., Davis, M. E., Bolzan, J. F., Dai, J., Yao, T., Gundestrup, N., Wu, X., Klein, L., Xie, Z.. Holocene-Late Pleistocene climatic ice core records from the Qinghai-Tibetan Plateau. Science, 1989, 246: 474-477.
[61] Fang, J. Q.. Lake evolution during the past 30,000 years in China, and its implications for environmental change. Quaternary Research, 1991, 36: 27-60.
[62] Li, S., Shi, Y.. Glacial and lake fluctuations in the area of West Kunlun mountains during the last 45,000 years. Annals of Glaciology, 1992, 16: 79-84.
[63] Owen, L.A., Windley, B.F., Cunningham, W.D., Badamgarov, G., Dorjnamjaa, D.. Quaternary alluvial fans in the Gobi of southern Mongolia: evidence for neotectonics and climate change. Journal of Quaternary Science, 1997, 12: 239-252.
[64] Zhang, H., Ma, Y., Wunnemann, B., Pachur, H.. A Holocene climatic record from arid northwestern China. Palaeogeography, Palaeoclimatology, Palaeoecology, 2000, 162: 389-401.
[65] Ye, W., Ji, F.. Comparision of paleoclimatic characteristics between monsoon and westerly areas, China. Chinese Science Bulletin, 2001, 46 (Supplementary): 119-124.
[66] Yang, X., Liu, T., Xiao, H.. Evolution of megadunes and lakes in the Badain Jaran Desert, Inner Mongolia, China during the last 31,000 years. Quaternary International, 2003, 104: 99-112.
[67] Zhu, B., Yang, X.. Chemical Weathering of Detrital Sediments in the Taklamakan Desert, Northwestern China. Geographical Research, 2009, 47: 57-70.
[68] Mischke, S., Herzschuh, U., Zhang, C., Bloemendal, J., Riedel, F.. A Late Quaternary lake record from the Qilian Mountains (NW China): lake level and salinity changes inferred from sediment properties and ostracod assemblages. Global and Planetary Change, 2005, 46: 337-359.
[69] Goudie, A. S.. Global deserts and their geomorphological diversity. In, Parsons, A.J., Abrahams A.D., (Eds.). Geomorphology of Desert Environments. Springer Science + Business Media, 2009: 9-20.
[70] McFadden, L.D., Wells, S.G., Jercinovich, M.J.. Influences of eolian and pedogenic processes on the origin and evolution of desert pavements. Geology, 1987, 15: 504-508.

  DOI: https://doi.org/10.30564/jgr.v2i1.1942

[71] Feng, Z.. Gobi dynamics in the Northern Mongolian Plateau during the past 20,000+ yr: preliminary results. Quaternary International, 2001, 76/77: 77-83.

[72] Zhang, H., Ming, Q., Lei, G., Zhang, W., Fan, H., Chang, F., Wunnemann, B., Rtmann, K.. Dilemma of dating on lacustrine deposits in a hyperarid inland basin of NW China. Radiacarbon, 2006, 48: 219-226.

[73] Lv, Y., Gu, Z., Ala, A., Zhang, H., Goran, P., Lei, G.. 10Be in quartz gravel from the Gobi Desert and evolutionary history of alluvial sedimentation in the Ejina Basin, Inner Mongolia, China. Chinese Science Bulletin, 2010, 55: 3802-3809.

[74] XETCAS (Xinjiang Expedition Team of the Chinese Academy of Sciences), IGCAS (Institute of Geography of the Chinese Academy of Sciences), DGBNU (Department of Geography of Beijing Normal University). Geomorphology in Xinjiang. Beijing, Science Press, 1978 (in Chinese).

[75] Oguchi, T., Saito, K., Kadomura, H., Grossman, M.. Fluvial geomorphology and paleohydrology in Japan. Geomorphology, 2001, 39: 3-19.

[76] Wunnemann, B., Pachur, H., Li, J., Zhang, H.. The chronology of Pleistocene and Holocene lake level fluctuations at Gaxun Nur/Sogu Nur and Baijian Hu in Inner Mongolia, China. Petermanns Geographische Mitteilungen, 1998, 142: 191-206.

[77] Jin, M., Li, G., Li, F., Duan, Y., Wen, L., Wei, H., Yang, L., Fan, Y., Chen, F.. Holocene shorelines and lake evolution in Juyanze Basin, southern Mongolian Plateau, revealed by luminescence dating. The Holocene, 2015, 25: 1898-1911.

[78] Li, G., Jin, M., Duan, Y., Madsen, D.B., Li, F., Yang, L., Wei, H., Chen, F.. Quartz and K-feldspar luminescence dating of a Marine Isotope Stage 5 megalake in the Juyanze Basin, central Gobi Desert, China. Palaeogeography Palaeoclimatology Palaeoecology, 2015, 440: 96-109.

[79] Chen, F., Wu, W., Holmes, J.. A mid-Holocene drought interval as evidenced by lake desiccation in the Alashan Plateau, Inner Mongolia China. Chinese Science Bulletin, 2003, 48: 1401-1410.

[80] Chen, F., Yu, Z., Yang, M.. Holocene moisture evolution in arid central Asia and its out-of-phase relationship with Asian monsoon history", Quaternary Science Reviews, 2008, 27: 351-364.

[81] Wunnemann, B., Hartmann, K., Altmann, N., Hambach, U., Pachur, H. J., Zhang, H.. Interglacial and Glacial fingerprints from lake deposits in the Gobi Desert, NW China. Developments in Quaternary Sciences, 2007b, 7: 323-347.

[82] Yu, J., Kelts, K.R.. Abrupt changes in climatic conditions across the late-glacial/Holocene transition on the N.E. Tibet-Qinghai Plateau: Evidence from Lake Qinghai, China. Journal of Palaeolimnology, 2002, 28: 195-206.

[83] Yu, Y., Yang, T., Li, J.. Millennial-scale Holocene climate variability in the NW China drylands and links to the tropical Pacific and the North Atlantic. Palaeogeography Palaeoclimatology Palaeoecology, 2006, 233: 149-162.

[84] Zhang, H., Peng, J., Ma, Y.. Late quaternary palaeolake levels in Tengger Desert, NW China. Palaeogeography Palaeoclimatology Palaeoecology, 2004: 211, 45-58.

[85] Norin, E.. Sven Hedin Central Asia Atlas. Memoir on maps, Stockholm, 1980.

[86] Hartmann, K., Wunnemann, B.. Hydrological changes and Holocene climate variations in NW China, inferred from lake sediments of Juyanze palaeolake by factor analyses. Quaternary International, 2009, 194: 28-44.

[87] Benn, D., Owen, L.. The role of the Indian summer monsoon and the mid-latitude westerlies in Himalayan glaciation: review and speculative discussion. Journal of Geological Society London, 1998, 155: 353-363.

[88] Grunert, J., Lehmkuhl, F., Walther, M.. Palaeoclimatic evolution of the Uvs Nuur basin and adjacent areas (Western Mongolia). Quaternary Internation, 2000, 65/66: 171-192.

[89] Yang, X., Preusser, F., Radtke, U.. Late Quaternary environmental changes in the Taklamakan Desert, western China, inferred from OSL-dated lacustrine and aeolian deposits. Quaternary Science Reviews, 2006, 25: 923-932.

[90] An, Z., Wu, X., Lu, Y., Zhang, D., Sun, X., Dong, G., Wang, S.. Paleoenvironmental changes of China during the last 18,000 years. In, Liu, T. (Ed.). Quaternary Geology and Environment in China. Beijing, Science Press,1991: 228-236.

[91] Ding, Z., Liu, T., Rutter, N. W., Yu, Z., Guo, Z., Zhu, R.. Ice volume forcing of Asian winter monsoon variations in the past 800,000 years. Quaternary Research, 1995, 44: 149-159.

[92] Pachur, H.J., Wunnemann, B., Zhang, H.C.. Lake evolution in the Tengger Desert, northwestern China, during the last 40,000 years. Quaternary Research, 1995, 44: 171-180.

[93] Herzschuh, U., Tarasov, P., Wunnemann, B., Hartmann, K.. Holocene vegetation and climate of the Alashan Plateau, NW China, reconstructed from pollen data. Palaeogeography Palaeoclimatology Palaeoecology, 2004, 211: 1-17.

BILINGUAL PUBLISHING CO.
Pioneer of Global Academics Since 1984

Journal of Geological Research
https://ojs.bilpublishing.com/index.php/jgr-a

ARTICLE

The Application of Geophysical Techniques in Tracking Leachate Plumes Migration in a Typical Cemetery within the Sandy formation in Benin City, Nigeria

Idehen, Osabuohien[1*] **Alile Owens Monday**[2] **Airen O. John**[2]

1. College of Education, Ekiadolor-Benin, Nigeria
2. University of Benin, Nigeria

ARTICLE INFO

Article history
Received: 9 June 2020
Accepted: 19 June 2020
Published Online: 30 June 2020

Keywords:
Geophysical
Tracking
Leachate
Migration
Cemetery

ABSTRACT

The survey aim is to track leachate plumes within the sandy formation which is below the surface laterite layer. It investigates the presence and migration of leachate plumes in the sandy region in a typical cemetery (Third Cemetery), in Benin City, Nigeria. The research engaged Vertical Electrical Sounding (VES), 2-Dimensional computation of migration in both the vertical and horizontal directions. The electrical resistivity data collected in parallel equidistant lines was processed to obtain geo-electric models using Res2dinv. The leachate plumes in the cemetery migrate vertically and horizontally at different rates. The maximum and minimum rates of vertical migration are 4.1 and 0.2 cm/day respectively, while the maximum and minimum rates of horizontal migration are 32.8 and 1.7 cm/day respectively. Volumetric analysis of the plume zones indicates that of the 75,231m^3 of the subsurface imaged, 6,322 m^3 is the zone contaminated by leachate plume, that is, 8.4 % of the earth volume investigated contained leachate plume. The research also showed that repeated ERT surveys can track movement of leachate plume emanating from decomposed dead bodies over time in active cemetery. The average travel time for a leachate plume to transverse a vertical distance of 6.6 m in coarse sand is 366.7 days at constant migration speed of 1.8 cm/day.

1. Introduction

Interment of bodies in cemeteries remains a widespread practice and the only alternative endpoint to dead bodies in Nigeria. In Benin City and Nigeria in general, the major cemeteries are located close to human residential areas and virtually all the populace within this locality depends on groundwater as the primary water source for various domestic purposes [1]

Many countries do not have appropriate legal regulations with regards to location of cemeteries. If not appropriately located or not sufficiently protected, cemeteries pose a significant health problem for the people [2]. Health concern about possible impact of the cemeteries in Nigeria on the water supply has prompted this research. According to DOC [3], cemetery sites/graveyards have the potential to result in impact on the local water environment and in particular, the groundwater underlying such sites. Multiples of studies elsewhere in the world have been devoted to impact of interment of bodies in cemeteries to

**Corresponding Author:*
Idehen,
Osabuohien, College of Education, Ekiadolor-Benin, Nigeria;
Email: idehenosabuohien@gmail.com

DOI: https://doi.org/10.30564/jgr.v2i1.1970

the groundwater quality [4-11]. Toxic chemicals that may be released into groundwater include substances that were used in embalming and burial practices as well as varnishes, sealers and preservatives and metal component of ornaments used on wooden coffins [12]. Wood preservatives and paints used in coffin construction contain compounds such as copper, naphthalene and ammoniac or chromated copper arsenate [13]. Paints contain lead, mercury, cadmium, and chromium; arsenic is used as a pigment, wood preservative and anti-fouling ingredient while barium is used as a pigment and a corrosion inhibitor [14,15].

Studies on the impact of cemeteries on the quality of groundwater in unsaturated and saturated zones are usually conducted within or at some distance from the cemeteries [16]. Over 40% of cemeteries in South Africa contaminate water resources. Local authorities seem oblivious of the problem. Both legal regulation and the determination to act in a way which would limit the threat are lacking [17].

2. Study Area

This study was conducted in Benin City located in south-south geopolitical zone of Nigeria. Benin City is bounded by latitudes 06° 06' N, 06° 30' N and longitudes 005° 30' E, 005° 45' E and an area of about 500 square kilometers [18]. The city is located within the rain forest ecological zone with annual mean temperature of 27.5 °C [19] and an annual mean rain fall of about 2095 mm [20]. Three cemeteries namely First, Second and Third cemeteries are located within this city. The Third cemetery which has existed for over 50 year was considered for this study because of its proximity to human residents. The cemetery which is the biggest among the cemeteries in Benin City covers an area of about 5.167 ha [21].

Geological sitting of Benin City is underlain by sedimentary formation described by [22]. The formation is made up of top reddish clayey sand capping highly porous fresh water bearing loose pebby sands, and sandstone with local thin clays and shale interbeds.

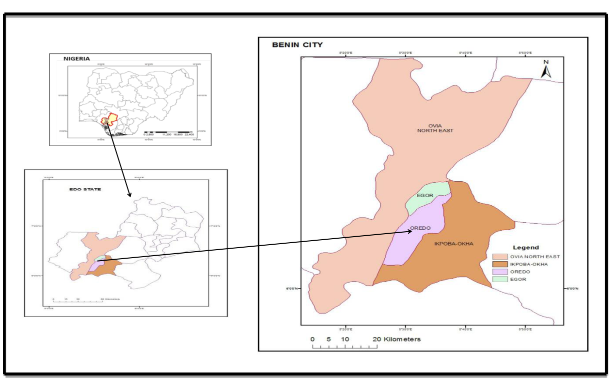

Figure 1. Study Area Map Showing Benin City with Four Local Government Areas

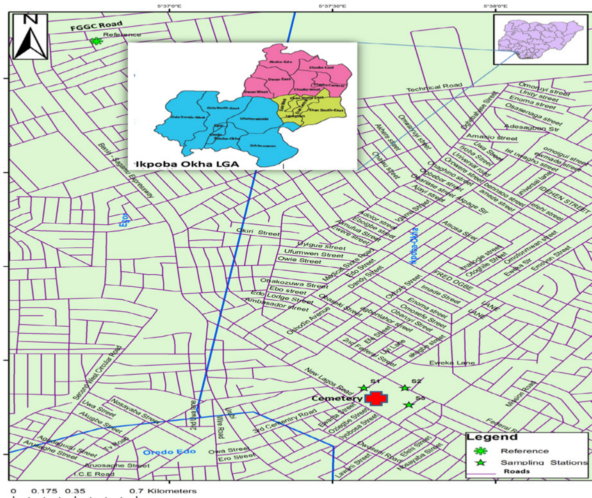

Figure 2. Map of Study Area (Third Cemetery). [23]

3. Methodology

Electrical resistivity imaging data was acquired twice using Pasi Earth Resistivity Meter. The second data set was acquired six months after the first one. The data coverage was made over an area defined by rectangular loop measuring 30m by 230m in the first survey while in the second survey was 30m by 200m. The resistance values were read from the measuring instrument using Wenner -Schlumberger array. This array is moderately sensitive to both horizontal structure and vertical structures [24].

In first survey, in each line location, electrodes numbered 0- 23 were placed into the ground at intervals of 10m along the line, while in the second survey, electrodes numbered 0-40 at 5m interval was planted into the ground. Each time measurement was to be taken, array of four electrodes are selected manually and connected to the Petrozenith earth resistivity meter via single core cable.

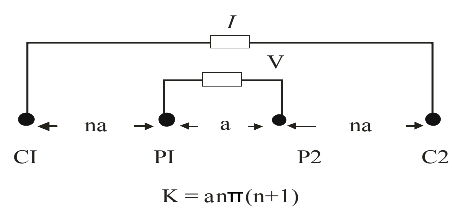

Figure 3. Wenner-Schlumberger Array [25]

$$K = an\pi(n+1) \tag{1}$$

$$\rho = KR \tag{2}$$

4. Data Processing and Interpretation

The electrical resistivity data was processed to obtain geoelectric models using Res2dinv and the second -survey data set was also merged and inverted as a single 3-D data set using Res3Dinv software, which is then visualized in detail using Voxler 4.0. The processed data depicted clearly the locations of low resistivity (blue) which occur at depths below 5.19m and 2.60m in the first and second surveys (subsurface data collection started at these depths) that are most likely to indicate accumulation of leachate plumes.

5. Discussion of Geophysical Tomography

The survey aim is to track leachate plumes within the sandy formation which is below the surface laterite layer. The sandy formation is a graded sand bed as seen from lithology log obtained from an existing borehole in vicinity. The water table likely occurs between the very coarse sand and medium sand. As leachate plume is detected in the medium sand, water in the well sorted coarse sand will be contaminated. If this shallow aquifer is polluted, there is high probability that the nearby deep confined, coarse sand aquifer at depth of 60 m (200 ft) is at risk. The geoelectric models obtained for the first and second surveys displayed leachate plumes starting from the laterite (the burial environment) down to the sandy formation (the regional water supply source). The leachate plumes presence in the sand bed are modeled and described as shown in the 2-D and 3-D displays, (Figure 4 to Figure 9) and Table 1.

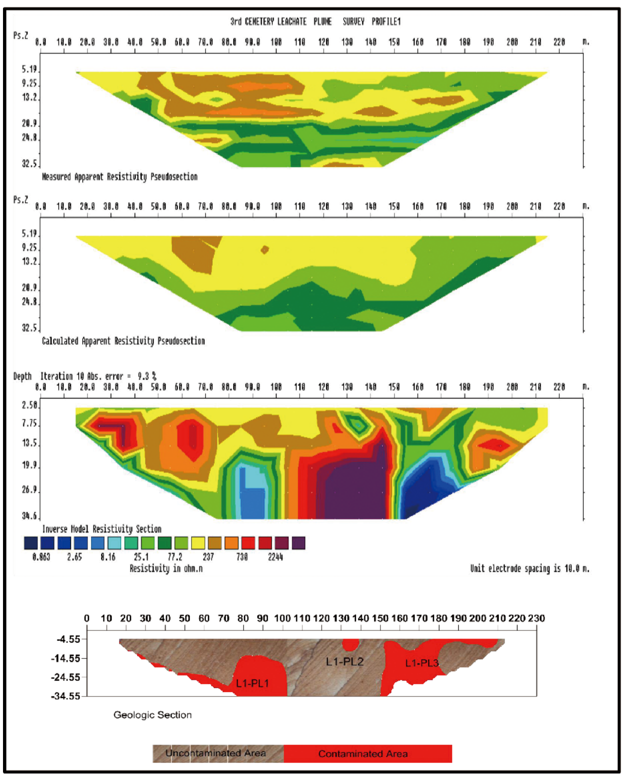

Figure 4. First Survey Profile 1

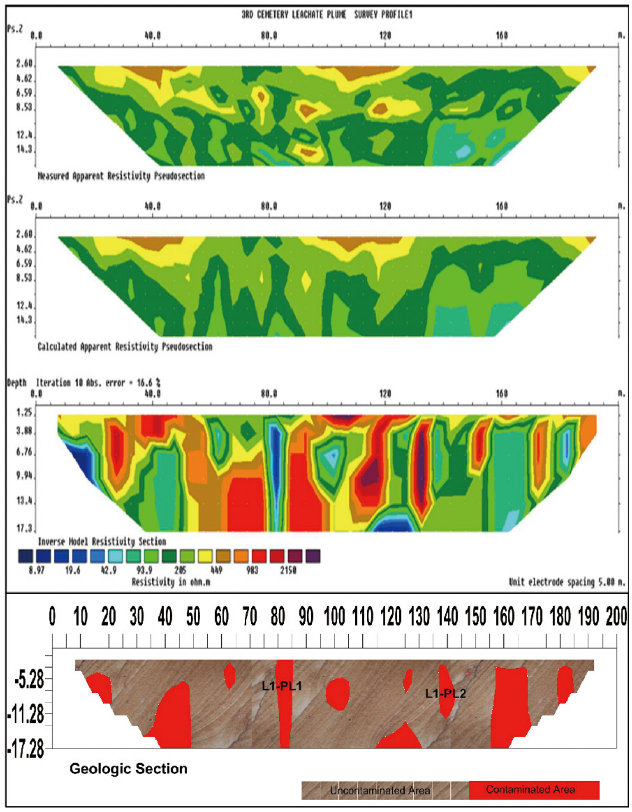

Figure 5. Second Survey Profile 1

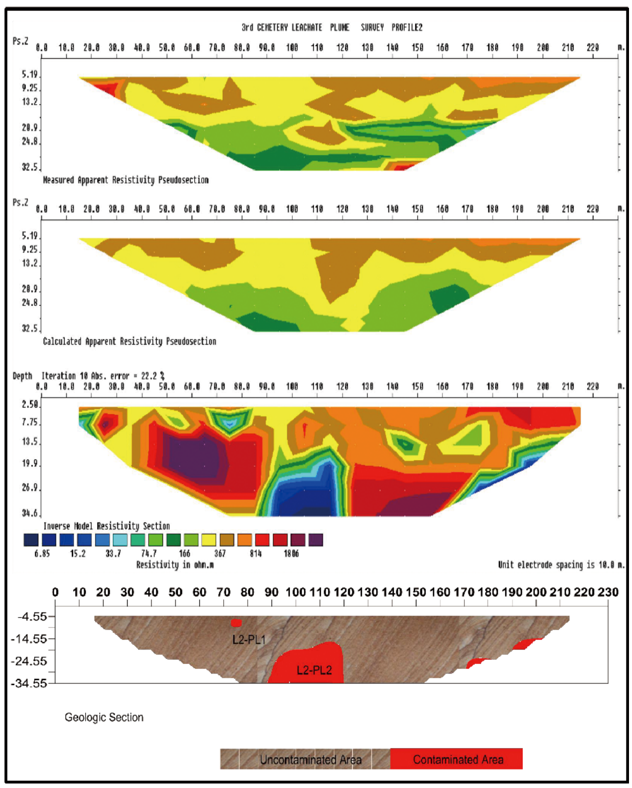

Figure 6. First Survey Profile 2

DOI: https://doi.org/10.30564/jgr.v2i1.1970

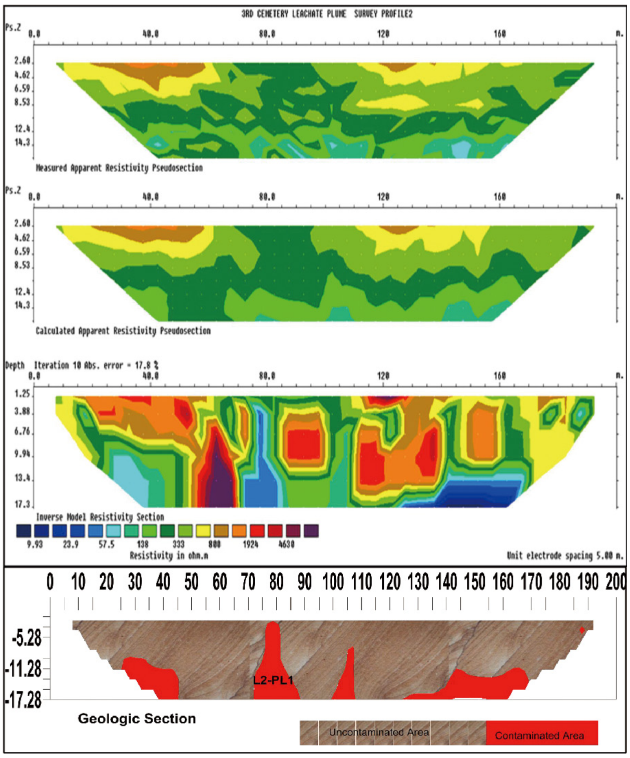

Figure 7. Second Survey Profile 2

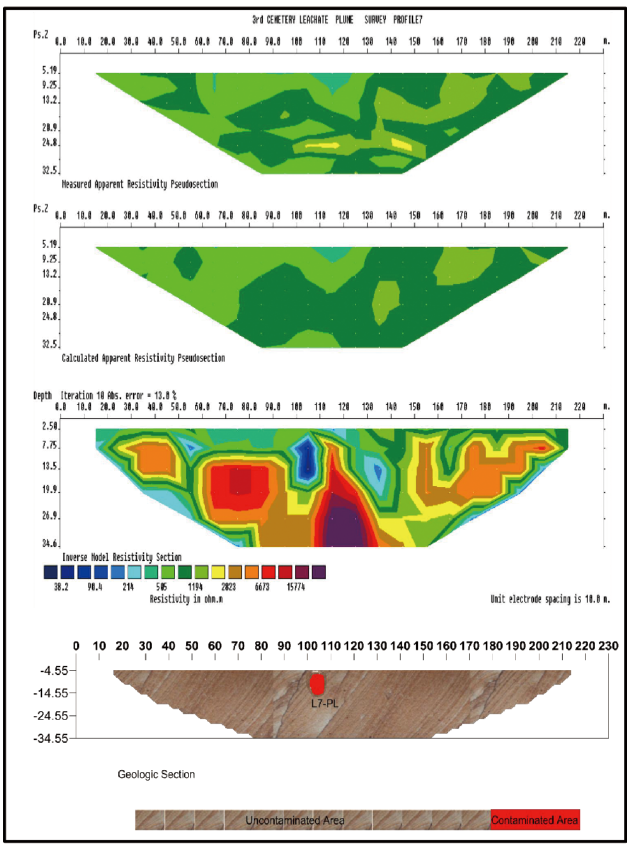

Figure 8. First Survey Profile 7

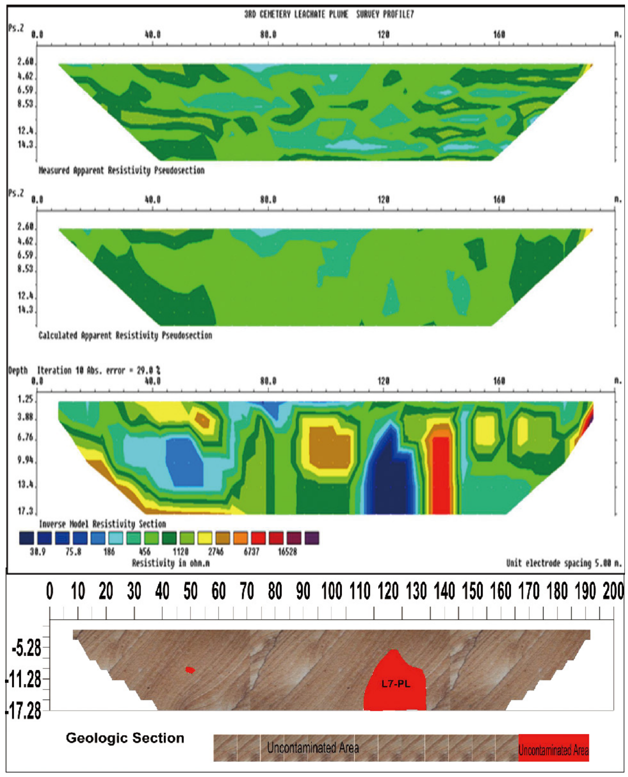

Figure 9. Second Survey Profile 7

6. Discussion of Time Lapse

The field works were conducted in two sessions with a time interval of six (6) months. The first ERT survey was conducted in June 2017 (early period of rainy season) and the second ERT survey was conducted in December 2017 (early period of dry season) when the plumes must have been diluted with excess infiltrating water and move faster in the vertical and horizontal directions. The rate of migration depends on the permeability of the soil, incline topography, depressions created by decomposed corpses and collapsed burial materials. All these aid infiltration into the subsurface.

The rate of migration in the horizontal direction is higher than the rate of migration in the vertical direction as shown in Table 1. The maximum rate of migration in the vertical direction is 4.1 cm/day while the maximum rate of migration in the horizontal direction is 32.8 cm/day. From the Table 1, it is observed that horizontal migration is higher than the corresponding vertical migration. The plume flows vertically and outwardly into the ground, and the horizontal permeability of sediment is found to be higher than the vertical permeability except in vertical solution fractures [26].

Table 1. Time Lapss Analysis

	June, 2017			*Dec. 2017*				*Vert. Shift (m)*	*Horiz Shift (m)*	*Vert. Migrat. Rate (cm/day)*	*Horiz. Migrat. Rate (cm/day)*
Plume	**Average Resist. (Ωm)**	**Bottom Depth (m)**	**Horiz Extent (m)**	**Plume**	**Average Resist. (Ωm)**	**Bottom Depth (m)**	**Horiz. Extent. (m)**				
L1-PL2	61	10	10	L1-PL2	94	12	13	2.0	3	1.1	1.7
L2-PL1	51	10	3	L2-PL1	73	17.3	20	7.3	17	4.1	9.4
L3-PL1	76	14.5	10	L3-PL1	52	17.3	20	2.8	10	1.6	5.6
L3-PL2	89	17	1	L3-PL2	79	17.3	60	0.3	59	0.2	32.8
L4-PL4	97	14	5	L4-PL	63	13.6	25	0.4	20	0.2	11.1
L7-PL	64	14	4	L7-PL	31	17.3	25	3.3	21	1.8	11.7

Plume, L2-PL1 has the highest vertical migration rate (4.1cm/day), and found in the very coarse sand bed as seen from the nearby borehole lithology log. This could however enhance the migration rate by virtue of the sediment high porosity and permeability. Water producing borehole within or close to this sand unit is probably at the point of contamination.

The borehole lithology log made at vicinity of the cemetery revealed that very coarse sand occurs at the depth range 32 ft (9.6 m) to 72 ft (21.6 m). The plume, PL7-PL has the highest migration rate (1.8 cm/day) and depth to the bottom is 17.3 m (58 ft). The sand bed is graded one: porosity and permeability differ, and hence fluid flow rate differ. Assuming the flow of Plume, PL7-PL within the environment of occurrence (very coarse sand) is at constant speed, and then the migration can be modeled in the form:

$$H=1.8T \tag{3}$$

$$T = H/1.8 \tag{4}$$

H= Distance traveled. T= Time taken.

The plume occurs at 22 ft (6.6 m) or 660 cm away from bottom of the very coarse sand. The time it may take the plume to transverse a distance of 6.6 m within the sand is

T= 660/1.8 = 366.7 days (approx. year).

The leachate plumes interpreted from the 2-D vertical display were located in the 3-D distribution plot using their depths of occurrence and lateral locations on the 2-D survey profiles. The volumetric analysis (carried out at the Voxler4.0 window) of the plume zones indicate that, out of 75,231 m^3 of the subsurface visualized, 6,322 m^3 is the zone contaminated by leachate plume, that is, 8.4% of the earth volume investigated contain leachate plume [27].

7. Conclusion

The survey aim is to track leachate plumes within the sandy formation which is below the surface laterite layer. Under favourable hydrological and geological conditions, the plumes delineated from the Electrical Resistivity Imaging will slowly migrate into the groundwater. The maximum migration rates in the vertical and horizontal directions are 4.1 and 32.8 cm/day respectively.

Geophysical Methods employed in the investigations of leachate plume migration in Third Cemetery showed that the arrival time of the plumes to the next layer (within the sandy layer) of distance 6.6 m is 366.7 days, assuming the time rate is constant.

References

[1] Idehen, O. Time Lapse Geoforensic Investigation of Leachate Plume Migration from Active Cemetery in Benin City, Nigeria.Ph.D Thesis, University of Benin, 2018.

[2] Fisher, G. J., Croukamp, L.. Ground Water Contamination and its Consequences, Resulting from the Indiscriminate Placing of Cemeteries in the Third World Context. Conference Africa Needs Groundwater. University of the Witwatersrand, Johannesburg, South Africa, 1993.

[3] DOC. Cemeteries, Burials and the Water Environment;A good practice guide for applicants and planning authorities when planning cemetery developments or extensions. Practice guide. Version 1.1. NIEA Natural Heritage Division, Belfast BT7 2JA, 2016.

[4] Migliorini, R. B.. Cemeteries as source of pollution in aquifers.Study of the Vila Formosa cemetery in the sedimentary basin of São Paulo. MSc Dissertation, Instituto de Geociências, Universidade de São Paulo, São Paulo, 1994: 74.

[5] Formanek, P. A.. An assessment of groundwater contamination at cemetery sites method and case study. MSc. Dissertation, Queen's University Kingston, Ontario, Canada, 1997, 242: 635.
http://dx.doi.org/10.1007/s10745-014-9665-5

  DOI: https://doi.org/10.30564/jgr.v2i1.1970

[6] Ucisik, A. S., Rushbrook, P.. The impact of cemeteries on the environment and public health - an introduction briefing. WHO, Regional Office for Europe, World Health Organization. Rept. EUR/ICP/EHNA 01 04 01 (A), 1998: 1-11.

[7] Young, C. P., Blackmore, K. M., Leavens, A., Reynolds, P. J.. Pollution Potential of Cemeteries.Environment Agency England and Wales, 2002. Available online: https://www.gov.uk/government/uploads/system/uploads/attachment_data/file/290607/sprp2-024-1-e-e.pdf

[8] Dent, B. B.. Cemetery decay product profiles: two cases in Australian, unconsolidated, sandy aquifers, understanding Planet Earth. Searching for a Sustainable Future. 15th Australian Geological Convention, Abstracts, Sydney, 2000, 3-7: 130.

[9]. Hart A.. Ammonia shadow of my former self: a review of potential groundwater chemical pollution from cemeteries. Land Contamination & Reclamation, 2005, 13(3): 239-245.

[10]. Buckley, C.. Graveyards and Groundwater.International Association of Hydrogeologist Irish Group, 2012. Available online: http://www.iahireland.org/conferenceproceedings/2012.pdf

[11] Fineza, A. G., Marques, E. A. G., Bastos, R. K. X., Betim, L. S.. Impacts on the groundwater quality within a cemetery area in Southeast Brazil.Soils and Rocks, São Paulo, 2014, 37(2): 161-169.

[12]. Jonker, C., Olivier, J.. Mineral Contamination from Cemetery Soils: Case Study of Zandfontein Cemetery, South Africa. Int. J. Environ. Res. Public Health, 2012, 9: 511-520. DOI: 10.3390/ijerph9020511

[13] Spongberg, A. L., Becks, P.. Inorganic Soil Contamination from Cemetery Leachate. Water, Air, and Soil Pollution, 2000, 117: 313-327.

[14] Katz, S. A., Salem, H.. Chemistry and toxicology of building timbers pressure-treated with chromated copper arsenate: a review. J. Appl. Toxicol., 2005, 25: 1-7.

[15] Huang, S. L., Yin, C. Y., Yap, S. Y.. Particle size and metals concentrations of dust from a paint manufacturing plant. J. Hazard. Mater., 2010, 174: 839-842.

[16] Zychowski, J., Lach, J., Kolber, M.. Physico-chemical features of groundwaters on cemeteries of south-eastern Poland, in Burchard, J. (ed.), State and anthropogenic changes of water quality in Poland, 2000, 1: 261-269.

[17] Alfoldi, L., Croukamp, L.. Problems and biological treatment, state of the art report. Watscitech, 1988, 20(3): 1-131.

[18] Ikhuoria, I. A.. Urban land use patterns in traditional Nigeria City: A case study of Benin City. Land use policy, Great Britain, 1987, 4(1): 62-75.

[19] Ikhile, C. I., Oloriode, D. O.. Impact of climate change on underground-water resources development in Benin-Owena River basin, Edo State, Nigeria: case study. European Journal of Scientific Research, 2011, 63(2): 272 - 278.

[20] Ibhadode, C. A. E., Dirius, A. R., Akhimien. Adequacy or otherwise of cemetery space for sustainable human body disposal in Benin City, Nigeria. Ethiopian Journal of Environmental Studies & Management, 2017, 10(5): 566 - 571.

[21] Short K., Stauble A. J.. Outline of the Geology of Niger Delta. Am Assoc Petroleum Geologists Bull, 1967, 51: 761.

[22] Idehen, O., Ezenwa, IM.. Influence of Third Cemetery Location on the Quality of Domestic and Groundwater Resources in Benin City, Nigeria. Journal of Applied Sciences and Environmental Management. 2019, 23(1): 05-11, ISSN: 1119-8362. DOI: https://dx.doi.org/10.4314/jasem.v23i1.1

[23] Loke, M. H..Tutorial: 2-D and 3-Delectrical imaging surveys, 2004. Available at: www.geotomosoft.com

[24] Anthony Ravindran, A. I., Mohd. Abdul Kadar Prabhu H.. Groundwater Exploration Study using Wenner-Schlumberger Electrode Array through W-4 2D Resistivity Imaging Systems at Mahapallipuram, Chennai, Tamilanadu, India. Research Journalof Recent Sciences, 2012, 1(11): 36-40.

[25] Djebbar, T., Erle C., Donaldson. Petrophysics : theory and practice of measuring reservoir rock and fluid transport Properties, 2004.

[26]. Idehen O.. Volumetric Analysis of 3-D Resistivity Distribution of Leachate Plume in Third Cemetery, Benin, South-South, Nigeria. Journal of Advances in Physics. 2020, 17: 32-40. ISSN: 2347 - 3487. DOI: https://doi.org/10.24297/jap.v17i.8486

BILINGUAL PUBLISHING CO.
Pioneer of Global Academics Since 1984

Journal of Geological Research
https://ojs.bilpublishing.com/index.php/jgr-a

ARTICLE

Analysing the Influencing Factors of a Postgenetic Subsidence Doline's Development Using Model Experiments

Szilárd Vetési-Foith*

Faculty of Sciences, University of Pécs, 7624, Hungary

ARTICLE INFO

Article history
Received: 16 June 2020
Accepted: 26 June 2020
Published Online: 30 June 2020

Keywords:
Model experiment
Subsidence doline
Influencing factors
Connection between the parameters
Estimating other parameters

ABSTRACT

The subsidence dolines are the most common surface forms of the concealed karsts. One type of these dolines is the suffosion doline. In this model experiment the influential role of these kind of dolines' development factors were analyzed. The aim of the study was to determine the significance of the parameters (cover thickness, secondary porosity of the bedrock, chimney diameter, grain size) that influence the development of a suffosion doline. To study the influencing factors numerous (162) experiments were made with different parameters, in a manner that during the experiments we changed only one parameter, so the effects of it would be detectable from the final solution. These measurements were made with the use of a special tool, designed and built for this purpose. According to the data we gained from the model experiments, the development of a suffosion doline is influenced by many parameters. If these parameters are in an optimal connection to each other, a suffosion doline may appear on the surface. Knowing these parameters of the covered karstic depressions lets us estimate other parameters that may influence the development of the subsidence dolines.

1. Introduction

The objective of our study was to laboratically determine the parameters (size and diameter of the chimney, cover's thickness, grain size and the secondary porosity of the cover) which affect the development of the suffosion dolines and how these factors influence the simulations made by us. Numerous experiments were made with different parameters, in a manner that during the measurements we changed only one parameter at a time, so their impact to the final solution would be detectable. According to the data we gained from the model experiment we estimated some other parameters that influence the development of covered karstic depressions.

As of the middle 60's the use of model experiments gained popularity in karstic researches as well. We can find data in numerous papers which describe studying karstfields and karstsystems with model experiments [1,2,3]. In these researches plaster were used by the researchers instead of limestone. The reason of this was that the dissolution and the morphogenesis happens faster on plaster than on limestone. Before the millenium these kinds of experiments were concentrated mostly on the microforms (karren) of the coverless surface. The development of the rillenkarren was examined by Glew and Ford [4], the development of the wall karren was researched by Dzulinsky et al. [5]. The morphogenesis of the karrforms was examined by Veress et al. [6] using physical analogue model expe-

**Corresponding Author:*
Szilárd Vetési-Foith,
Faculty of Sciences, University of Pécs, Pécs Ifjúság str. 6, 7624, Hungary;
Email: szilard.vetesi@gmail.com

  DOI: https://doi.org/10.30564/jgr.v2i1.1988

riments, built on plaster as well. The dissolution, flow, sedimentation and subsidence processes under laboratory conditions on bare and covered karsts were examined by Veress and Péntek [7] and Deák et al. [8,9,10].

The model experiment discussed below is an upgrade of a method featured in two previous studies. In a model experiment presented by Veress et al. [11] the researchers put a covering layer with different grain sizes on individual plaster blocks and they studied the phenomenon developed on the cover by changing the place where the water was added. They stated that the size of the feature which formed on the cover's surface was specified by the nature of the water's movement as well as the size of the material loss in the bedrock. Vetési-Foith [12] analysed if porosity change in the cover induces the development of covered karstic depressions.

A similar process was analyzed by Arevalo and Zuriguel [13] in case of grain silos. The size of the lowering caused by gravitation, the size of the outlet, and the grain size were compared, and they measuered that, how the connection between these parameters cause clogging of the outlet. They stated, in the clogging of the outlet, the size of the outlet and the grain size has the biggest influential role. Nevertheless the size of the lowering caused by gravitation does not play a significant role in the process.

Depressions develop in natural conditions if the superficial deposit loses its stability [14]. Subsidence dolines can form by suffosion (suffosion doline), collapse (dropout doline), dissolution (solution doline) and compaction (compaction doline) [15,16,17,18]. Although these processes often work together.

On covered karst (concealed karst) subsidence dolines are the most characteristic landforms [19,20,16]. The subsidence dolines form during the rearrangement and material loss of the superficial deposit where the bedrock has a high or increased secondary porosity. This causes, that a part of the superficial deposit transports locally to the bedrock. The matter reciever forms can be the depressions of the bedrock, the branches of the the epikarst and the phreatic zone, and the cavities or branches of the superficial deposit as well [16,18,21].

If the superficial deposit is non-cohesive the matter of the cover transports into these dissolving forms of the bedrock either by suffosion or by shedding gradually. If the superficial deposit is cohesive it collapses into them if it loses its stability. The stability of the superficial deposit depends on its thickness, its clay content, the size of the cavities in it, the groundwater flow rate, the pressure of the pore water [14], the water abstraction, but it is affected by construction, vehicle traffic [16], point-increased load [22] as well. The material loss in the superficial deposit will cause a closed depression on it's surface.

A prerequisite for the processes above is that the bedrock must have material-absorbing capacity, i.e. secondary porosity. This is possible if, during its karstification, caves, shafts, chimneys, branches, karren, or other cavities form [15,23,24,25,20,16,18].

Subsidence dolines can be syngenetic and postgenetic [18]. The developed form on the superficial deposit and the form of the bedrock which receives the cover's material are coevals in case of syngenetic dolines, the receiver form of the bedrock is older by postgenetic dolines. The development of postgenetic depressions were modeled in our experiments.

The relationship between the thickness of the superficial deposit and the size of the subsidence dolines formed on it has been studied by several researchers. According to Waltham et al. [16] when the superficial deposit is thicker the dolines form on it are smaller. Hyatt et al. [26] suggest that doline size does not depend on the thickness of the superficial deposit or its water permeability, but rather on the type and age of it. In the following study, we did not simulate the formation of depressions, but examined the relationship between the thickness of the superficial deposit and the absorption capacity of the bedrock. The formation of subsidence dolinas is influenced by several processes, but the depressions of the present model experiment were developed exclusively by grain shedding and the role of the studied parameters was studied on this basis. Although the dolines measured in this study are characteristic landforms of clayey superficial deposit, its use was omitted because the cohesiveness of the clay would have prevented the process of grain shedding.

During the experiments (covered karstic environment in a laboratory and simulated processes) we are looking for answers to the following questions:

(1) Is the volume of the material loss in the superficial deposit (henceforward cover) equal to the volume of the depression on the cover's surface?

(2) If not, what causes the difference?

(3) How are the parameters of the depression on the cover's surface influenced by the cover's thickness, the diameter of the chimney, volume of the void space below the chimney and the grain size of the cover?

(4) How can we define the so-called active zone (see below) participating in the depression's formation, and what kind of parameters influence it's size?

(5) How can we describe the process of the depression's formation?

(6) Is there any relation between the grain size of the cover and the shape (diameter/depth) of the depression?

(7) Is the involved but not known parameter playing a

 DOI: https://doi.org/10.30564/jgr.v2i1.1988

role in the development of natural dolines estimable if the parameters of the depression developed during the model experiment are known?

2. Methods

The Grain-shedder Tool

The experimental tool is a rectangular prism restricted by metal plates (henceforward the grain-shedder tool) into which cover material was piled up. At the bottom side of this tool can the blocks representing the bedrock - made of an easily fabricable material (plaster) - be found. Into these blocks boreholes were made with different diameters (henceforward chimney). Onto these blocks air dried and fractionated cover was put with varied parameters (thickness and grain size) in a manner that the two solid parts (the drilled plaster block and the cover) could be separated from each other. To achieve this a metal plate was slipped into the experimental tool from the side. When the metal plate was suddenly removed it allowed the cover to reach the chimney, thus creating a grain-flowing process which, although not a suffosion, is similar to it (Figure 1). It is not suffosion because it was not the water moving the grain, but a similar effect because the grain flows through the chimney to the space below the plaster block. Therefore this system is called the grain-shedder tool. The tool was built in a manner that it should be approximately a hundred times smaller than the natural dimensions.

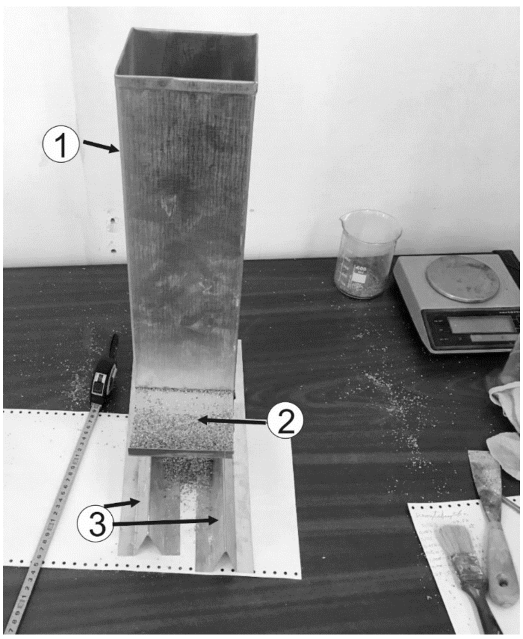

Figure 1. The experimental tool and it's parts, 1. the metal prism, 2. the metal plate what separates the drilled plaster block and the cover, 3. metal rails which create the void space below the tool

The experiments were made with the use of the grain-shedder tool using the following parameters:

(1) Diameter of the chimney: 0.5 cm, 1 cm, 1.5 cm.

(2) Cover thickness: 5 cm, 10 cm, 15 cm, 20 cm, 25 cm, 30 cm.

(3) Grain size of the cover: 0.250-0.500 mm, 0.500-1.000 mm, 1.000-2.000 mm.

(4) Without lifting the grain-shedder tool (0 cm), and with (2.5 cm and 5 cm) lifting the tool.

The space below the grain-shedder tool was necessary because there are many chimneys in natural karstic rocks below which there are horizontal cave systems (Figure 2).

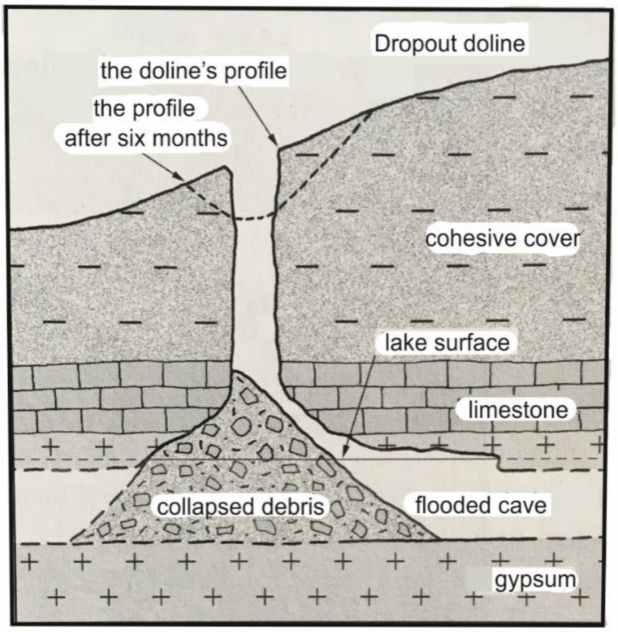

Figure 2. Horizontal cave system under a dropout doline [16]

The grain shedding phenomenon was studied in 162 experiments by combining these four parameters' different values. In each case we measured the lowering of the cover's surface, the diameter and the depth of the depression, as well as the volume of the material passed through the chimney. From these data further parameters were calculated. These are the followings:

(1) Volume of the depression (cm^3)

$$V_d=1/3*\pi*r^2*M_d \tag{1}$$

where V_d the volume of the depression (cm^3), r the radius of the depression (cm), M_d depth of the depression (cm). The established depressions were regarded as circular cones, thus for the calculating of the depression's volume we used the upper formula (Figure 3).

DOI: https://doi.org/10.30564/jgr.v2i1.1988

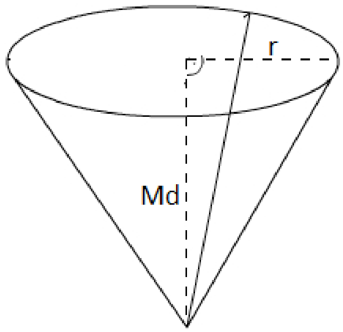

Figure 3. Theoretical figure of the created depression, r. radius of the depression, Md. depth of the depression

(2) The shape of the depression (O):

$$O=2r/M_d \qquad (2)$$

where r is the radius of the depression (cm), M_d means the depth of the depression (cm) (Figure 3).

(3) Volume of the active zone that participates in the formation of the depression ($V_{active\ zone}$):

$$V_{active\ zone}=1/3*\pi*r^2*h \qquad (3)$$

where r is the radius of the depression (cm), h is the cover's thickness at the end of the experiment (cm) (Figure 4).

During the experiments we stated that during the development of the depression an active- and a passive zone came into being. The active zone is the part of the cover from which the cover's material departs directly into the chimney. The passive zone is the part of the cover from which the cover's material doesn't depart through the chimney directly, but it may depart to the active zone (Figure 4).

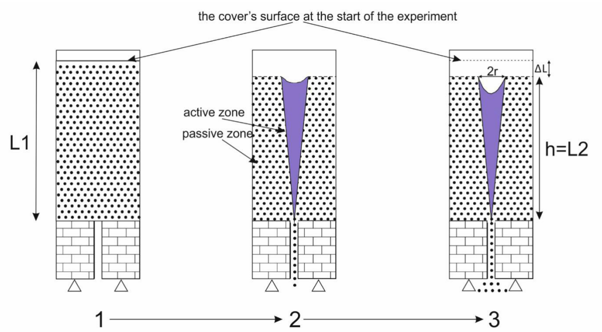

Figure 4. Flowchart of the depression's developing. 1. the start of the experiment, 2. the matter sheds through the chimney, 3. a depression formed on the cover at the end of the experiment, L1. thickness of the cover before the experiment, h=L2. thickness of the cover after the experiment, 2r. diameter of the depression, ΔL subsidence of the cover's surface

(4) The size of the active zone compared to the original volume of the cover (V_{az}%):

$$V_{az}\%=V_{az}/V_1 100 \qquad (4)$$

where V_{az} is the volume of the active zone (cm^3), V_1 is the original volume of the cover (cm^3), which we get as we calculated the volume of the cover in the grain-shedder tool.

(5) Estimating other, not known parameters of the covered karstic depressions:

For the estimatings quotients was made as the followings:

(1) The depth of the depression formed during the experiment was divided by the cover's thickness. If we know the quotient, the degree of the reduction and the depth of the natural depression, the cover's thickness involved in the formation is estimable.

(2) The diameter of the depression formed during the experiment was divided by the cover's thickness. If we know the quotient, the degree of the reduction and the diameter of the natural depression we are able to determine the cover's thickness involved in the formation.

3. Results

3.1 Relationship between the Material Loss Made in the Bedrock and the Volume of the Depression Formed on the Cover's Surface

During the grain sheddings two phenomenons were appearing on the cover's surface: the sagging of the whole surface and a depression occuring on a part of it. Based on the measured data we stated, that the volume of the depression formed on the cover's surface and the volume of the matter shedded through the chimney are not equal (table 1, 2 and 3). The volume of the matter shedded through the chimney was always greater than the volume of the depression. With the reduction of the cover's thickness the volume of the depression is getting closer to the volume of the fallen matter, but it never reaches its size. By 20 cm cover thickness and by 0.5 cm chimney diameter, with the use of the smallest grain size the volume of the fallen matter is 42 cm^3, the volume of the depression is 0.1 cm^3. With changing the cover's thickness the data changes as the followings: when the cover is 15 cm thick the volume of the flowed matter is 42 cm^3, the volume of the depression is 3.5 cm^3. When the cover is 10 cm thick the volume of the flowed matter is 43 cm^3 the volume of the depression is 13.1 cm^3. When the cover is 5 cm thick the volume of the shedded matter is 44 cm^3, the volume of the depression is 36.8 cm^3 (table 1).

 DOI: https://doi.org/10.30564/jgr.v2i1.1988

Table 1. A part of the data set, made by the data of the experiments 1

Lifting (cm)	Dk (cm)	Dsz (cm)	L1 (cm)	ΔL (cm)	ΔV (cm^3)	2r (cm)	Md (cm)	Accomplished?	Volume of the depression cm^3
2.5	0.5	0.250-0.500	5	0.4	44	7.5	2.5	yes	36.8
			10	0.8	43	5	2	yes	13.1
			15	1	42	3	1.5	yes	3.5
			20	1	42	1	0.5	yes	0.1
			25	1.2	43	N/A	N/A	yes	0
			30	1.3	44	N/A	N/A	yes	0
		0.500-1.000	5	0.4	14	1	0.5	yes	0.1
			10	0.3	10	N/A	N/A	no	0
			15	0.4	11	N/A	N/A	no	0
			20	0.3	11	N/A	N/A	no	0
			25	0.2	10	N/A	N/A	no	0
			30	0.2	10	N/A	N/A	no	0
		1.000-2.000	5	0	0	N/A	N/A	no	0
			10	0	0	N/A	N/A	no	0
			15	0	0	N/A	N/A	no	0
			20	0	0	N/A	N/A	no	0
			25	0	0	N/A	N/A	no	0
			30	0	0	N/A	N/A	no	0

Note: Dk. diameter of the chimney, Dsz. soil fractions, L1. thickness of the cover at the beginning of the experiment, ΔL. the amount of decrease of the cover's thickness, ΔV. the volume of the fallen matter, Md. depth of the depression

Table 2: A part of the data set, made by the data of the experiments 2

Lifting (cm)	Dk (cm)	Dsz (cm)	L1 (cm)	ΔL (cm)	ΔV (cm^3)	2r (cm)	Md (cm)	Accomplished?	Volume of the depression cm^3
2.5	1	0.250-0.500	5	0.4	61	9	2.8	yes	59.3
			10	0.5	63	8	2.2	yes	36.8
			15	0.5	63	7	2	yes	25.6
			20	0.9	55	2.5	1	yes	1.6
			25	1	55	1	0.5	yes	0.1
			30	1.2	62	N/A	N/A	yes	0
		0.500-1.000	5	0.8	54	5	2.5	yes	16.3
			10	1	56	2	1.5	yes	1.5
			15	1.3	54	N/A	N/A	yes	0
			20	1.2	55	N/A	N/A	yes	0
			25	1.2	55	N/A	N/A	yes	0
			30	1	55	N/A	N/A	yes	0
		1.000-2.000	5	0.5	8	1	0.5	no	0.1
			10	0.3	4	N/A	N/A	no	0
			15	0.1	2	N/A	N/A	no	0
			20	0.2	4	N/A	N/A	no	0
			25	0.1	2	N/A	N/A	no	0
			30	0.1	2	N/A	N/A	no	0

Note: Dk. diameter of the chimney, Dsz. soil fractions, L1. thickness of the cover at the beginning of the experiment, ΔL. the amount of decrease of the cover's thickness, ΔV. the amount of the fallen matter, Md. depth of the depression.

DOI: https://doi.org/10.30564/jgr.v2i1.1988

Table 3: A part of the data set, made by the data of the experiments 3

Lifting (cm)	Dk (cm)	Dsz (cm)	L1 (cm)	ΔL (cm)	ΔV (cm^3)	2r (cm)	Md (cm)	Accomplished?	Volume of the depression cm^3
2.5	1.5	0.250-0.500	5	0.2	84	9.5	2.8	yes	66.1
			10	0.4	83	8	3	yes	50.2
			15	0.4	84	8	2.5	yes	41.8
			20	0.6	88	7	3	yes	38.4
			25	0.8	85	4.5	2.8	yes	14.8
			30	0.9	86	3	1.5	yes	3.5
		0.500-1.000	5	0.6	78	7	2.8	yes	35.9
			10	0.8	78	6	2.5	yes	23.5
			15	0.8	77	4	2.2	yes	9.2
			20	0.9	78	3.8	0.5	yes	1.8
			25	1.1	78	N/A	N/A	yes	0
			30	1	78	N/A	N/A	yes	0
		1.000-2.000	5	0.4	68	7	3	yes	38.4
			10	0.6	67	2.5	2	yes	3.2
			15	1.3	67	N/A	N/A	yes	0
			20	1.2	68	N/A	N/A	yes	0
			25	1	68	N/A	N/A	yes	0
			30	0.8	68	N/A	N/A	yes	0

Note: Dk. diameter of the chimney, Dsz. soil fractions, L1. thickness of the cover at the beginning of the experiment, ΔL. the amount of decrease of the cover's thickness, ΔV. the amount of the fallen matter, Md. depth of the depression

3.2 The Effects of the Various Parameters' Values to the Development of the Depression

When the chimney's diameter is 0.5 cm the shedding took place only when we used the smallest grain size to build the cover. At 1 cm chimney diameter this process happens even with the use of the medium sized grains. When we built our model with the biggest chimney diameter (1.5 cm) we stated that the process of shedding takes place even with the use of the biggest grain size. Therefore the growth of the chimney's diameter allows material shedding even by a cover consisting of bigger grain, thus the formation of the depression as well. By some measurements we experienced that both the cover's thickness and the chimney's diameter impacts the shedding. Namely when we built our model with the use of 0.5 cm chimney diameter and with 5 cm thick cover, the process of shedding took place, however when the cover's thickness is 10 cm or bigger than that the grains are not able to get through the chimney. Accordingly by same sized chimney diameter and by thinner cover the process of shedding took place, on the other hand when the cover is thicker the shedding either doesn't start or the chimney is clogged during the shedding (table 1).

If the chimney's diameter is 1.5 cm, the cover's thickness is 5 cm then a depression of 66.1 cm^3 volume appears on the cover. With the same chimney diameter but thicker (10 cm) cover the volume of the formed depression is 50.2 cm^3. We stated that in contrast to the former (where the chimney's diameter was 1 cm), by 1.5 cm diameter a depression occured even on the model built with a 30 cm cover thickness (table 3).

The grain size has the following effects to the experiment: By a 1.5 cm chimney and 5 cm thick cover a 38.4 cm^3 depression occurs using the biggest (1.0-2.0 mm) grain. If the cover thickness is 10 cm with the other parameters unchanged, a 3.2 cm^3 depression develops. If the cover thickness is bigger than 10 cm, a depression will not appear in the same case. Using the smallest grain (0.250-0.500 mm) a depression of 3.5 cm^3 developed even on the thickest (30 cm) cover (table 3).

Without lifting the grain-shedder tool depressions occured only when we built the model with the thinnest cover. With lifting the grain-shedder tool space was created so the amount of material able to shed through was increased. Therefore a depression is able to occur not only at the thinnest, but even with the use of the thickest cover (table 3).

If all the parameters are examined together, then e.g. by 1.5 chimney diameter, with the use of the smallest (0.250-0.500 mm) grain size, a 30 cm thick cover, and the grain-shedder tool lifted to 2.5 cm, we experienced a depression with a volume of 3.5 cm^3. However if the

 DOI: https://doi.org/10.30564/jgr.v2i1.1988

chimney's diameter is only 1 cm and the other parameters are unchanged, there will be no depression on the cover's surface. Likewise there will be no depression on the cover's surface if the chimney's diameter is 1.5 cm, but we build the model with the use of the biggest grain size (1.0-2.0 mm) (table 2 and 3).

3.3 The Active Zone and Its Influencing Factors

We can speak about the active zone only in those cases when depression occurs on the cover's surface. In those cases when there is no depression the whole volume of the cover belongs to the passive zone. The volume of the active zone in itself does not give us an accurate view about its growth depending on the growth of the cover's thickness, thus the size of the active zone was compared to the given cover thickness and we have taken its percentage values as a basis.

According to the data the following parameters have influential role to the size of the active zone: the cover's thickness, the diameter of the chimney, the grain size of the cover, and the volume of the space under the chimney. Decreasing the cover's thickness and its grain size have a positive impact to the volume of the active zone, whereas decreasing the chimney's diameter and the volume of the space under the chimney have a negative impact to it.

By a 0.5 cm chimney diameter and the smallest grain size the volume of the active zone grows continously as the cover's thickness is decreasing. By a 1 and 1.5 cm chimney diameter using the same grain size the volume of the active zone grows continously until a certain point, then it starts to decrease. In spite of this decrease, the size of the specific active zone grows continously as the cover is thinning (table 5 and 6).

4. Discussion

4.1 Relation between the Material Loss made in the Bedrock and the Volume of the Depression Formed on the Cover's Surface

Since the volume of the material loss in the bedrock and the volume of the depression are not equal, thus we suppose that there are other processes during the forming of the depression, e.g. the compaction of the cover's material. This may be possible because during the shedding the grains get closer to each other.

The void volume of the cover is increasing at the be-

Table 4. A part of the data set, made by the data of the experiments

Lifting (cm)	Dk (cm)	Dsz (cm)	L1 (cm)	ΔL (cm)	ΔV (cm^3)	2r (cm)	Md (cm)	Volume of the active zone (cm^3)	Volume of the depression (cm^3)	Percentage values (%)
2.5	0.5	0.250-0.500	5	0.4	44	7.5	2.5	67.7	36.8	11.1
			10	0.8	43	5	2	60.2	13.1	4.9
			15	1	42	3	1.5	32.9	3.5	1.7
			20	1	42	1	0.5	4.9	0.1	0.2
			25	1.2	43	N/A	N/A	0	0	0
			30	1.3	44	N/A	N/A	0	0	0
		0.500-1.000	5	0.4	14	1	0.5	1.2	0.1	0.1
			10	0.3	10	N/A	N/A	0	0	0
			15	0.4	11	N/A	N/A	0	0	0
			20	0.3	11	N/A	N/A	0	0	0
			25	0.2	10	N/A	N/A	0	0	0
			30	0.2	10	N/A	N/A	0	0	0
		1.000-2.000	5	0	0	N/A	N/A	0	0	0
			10	0	0	N/A	N/A	0	0	0
			15	0	0	N/A	N/A	0	0	0
			20	0	0	N/A	N/A	0	0	0
			25	0	0	N/A	N/A	0	0	0
			30	0	0	N/A	N/A	0	0	0

Note: Dk. the diameter of the chimney, Dsz. soil fractions,, L1. thickness of the cover at the beginning of the experiment, ΔL. the amount of decrease of the cover's thickness, ΔV. the amount of fallen matter, 2r the diameter of the depression, Md. depth of the depression, Vd. volume of the depression.

DOI: https://doi.org/10.30564/jgr.v2i1.1988

Table 5. A part of the data set, made by the data of the experiments

Lifting (cm)	Dk (cm)	Dsz (cm)	L1 (cm)	ΔL (cm)	ΔV (cm^3)	2r (cm)	Md (cm)	Volume of the active zone (cm^3)	Volume of the depression (cm^3)	Percentage values (%)
2.5	1	0.250-0.500	5	0.4	61	9	2.8	97.5	59.3	15.9
			10	0.5	63	8	2.2	159.1	36.8	13.1
			15	0.5	63	7	2	186	25.6	10.1
			20	0.9	55	2,5	1	31.2	1.6	1.2
			25	1	55	1	0,5	6.2	0.1	0.2
			30	1.2	62	N/A	N/A	0	0	0
		0.500-1.000	5	0.8	54	5	2.5	27.4	16.3	4.4
			10	1	56	2	1.5	9.4	1.5	0.7
			15	1.3	54	N/A	N/A	0	0	0
			20	1.2	55	N/A	N/A	0	0	0
			25	1.2	55	N/A	N/A	0	0	0
			30	1	55	N/A	N/A	0	0	0
		1.000-2.000	5	0.5	8	1	0.5	1.1	0.1	0.1
			10	0.3	4	N/A	N/A	0	0	0
			15	0.1	2	N/A	N/A	0	0	0
			20	0.2	4	N/A	N/A	0	0	0
			25	0.1	2	N/A	N/A	0	0	0
			30	0.1	2	N/A	N/A	0	0	0

Note: Dk. the diameter of the chimney, Dsz. soil fractions,, L1. thickness of the cover at the beginning of the experiment, ΔL. the amount of decrease of the cover's thickness, ΔV. the amount of fallen matter, 2r the diameter of the depression, Md. depth of the depression, Vd. volume of the depression.

Table 6. A part of the data set, made by the data of the experiments

Lifting (cm)	Dk (cm)	Dsz (cm)	L1 (cm)	ΔL (cm)	ΔV (cm^3)	2r (cm)	Md (cm)	Volume of the active zone (cm^3)	Volume of the depression (cm^3)	Percentage values (%)
2.5	1.5	0.250-0.500	5	0.2	84	9.5	2.8	113.4	66.1	18.5
			10	0.4	83	8	3	160.8	50.2	13.1
			15	0.4	84	8	2.5	244.6	41.8	13.3
			20	0.6	88	7	3	248.8	38.4	10.1
			25	0.8	85	4.5	2.8	128.2	14.8	4.1
			30	0.9	86	3	1.5	68.5	3.5	1.8
		0.500-1.000	5	0.6	78	7	2.8	56.4	35.9	9.2
			10	0.8	78	6	2.5	86.7	23.5	7.1
			15	0.8	77	4	2.2	59.4	9.2	3.2
			20	0.9	78	3.8	0.5	72.2	1.8	2.9
			25	1.1	78	N/A	N/A	0	0	0
			30	1	78	N/A	N/A	0	0	0
		1.000-2.000	5	0.4	68	7	3	59	38.4	9.6
			10	0.6	67	2.5	2	15.3	3.2	1.2
			15	1.3	67	N/A	N/A	0	0	0
			20	1.2	68	N/A	N/A	0	0	0
			25	1	68	N/A	N/A	0	0	0
			30	0.8	68	N/A	N/A	0	0	0

Note: Dk. the diameter of the chimney, Dsz. soil fractions,, L1. thickness of the cover at the beginning of the experiment, ΔL. the amount of decrease of the cover's thickness, ΔV. the amount of fallen matter, 2r the diameter of the depression, Md. depth of the depression, Vd. volume of the depression.

ginning of the shedding because some matter gets from there to the active zone, followed by a compaction in the cover which is a process that can also cause the difference between the volume of the shedded matter and the volume of the depression (Figure 4). Because of this compaction the grains get closer to each other. This causes the areal sinking of the cover. The rate of the compaction is higher as the grain size is increasing, because in the cover made of bigger grains the grains are located farther from each other than in the cover consisting of small grains. The rate of the compaction is also getting higher with the thickening of the cover, because in the case of a thicker cover it's volume is bigger, thus the space between the grains is also bigger. This is adequately demonstrated: by decreasing the cover's thickness the rate of the areal sinking is decreasing as well. The areal sinking is decreasing because less material isn't able to compact that much.

4.2 The Effect of the Individual Parameters's Size to the Size of the Depression

The size of the depression and the possibility of its forming is affected by the chimney's diameter, the cover's thickness and its grain size, and the size of the space beneath the chimney. The volume of the space below the chimney has the greatest impact to the possibility of the depression's forming. The chimney's diameter is the other determinant of the forming. The bigger this parameter, the bigger the chance of the depression's forming. The grain size of the cover is the third determinant. For the smaller grains it is easier to shed through the chimney and they clog the chimney with a smaller chance, allowing the material to shed through. Considering the chance of the depression's forming the cover's thickness is a significant determinant as well.

The thicker the cover, the lower the chances of forming a depression. These parameters affect the forming of the depression by themselves and in an effect system in relation to each other as well. That's why none of the parameters can be examined in itself. Namely if there is no space underneath the chimney but the chimney's diameter is big, the grain size of the cover is small and all those parameters are coupled with a thin cover a depression can still occur. In this case if the chimney is fully filled with the cover's matter, it generates so big material loss in the cover that's enough for a small depression to develop. Although by increasing the space below the chimney a depression can still form even if the other parameters are less favorable to it's development (table 1, 2 and 3). Namely if the former is small, and the latter is big, then it doesn't matter how big the space below the chimney is the shedding will not start, because the big grains will clog the chimney preventing the matter to shed.

The size of the depression is definitely determined by the volume of the potential material loss. This depends mostly on the volume of the space below the chimney. The cover's thickness has the biggest influential role to the size of the depression. As the cover is even thinner the size of the forming depressions are increasing linearly. This can be attributed to that a material loss with the same volume at thin cover spreads to a cover with a smaller volume, so the material loss will be relatively bigger, because when the cover is thin less material can get from the passive zone to the active. For this bigger realive material loss the system responds with a bigger void volume growth, what causes relatively bigger compaction and so a higher rate of lowering.

4.3 The Active Zone and Its Influential Parameters

The volume of the active zone is lowering continously with the lowering of the cover's thickness (table 4, 5 and 6). Namely due to the matter-shedding, the void volume of the cover is increasing which is followed by a kind of compaction. The increase of the void volume will be bigger than the volume of the through-shedded matter. The thinner the cover this phenomenon shows up the more, so the increase of the void volume is followed by a bigger relative compaction.

4.4 The Process of the Depression's Forming

The forming of the depression is caused by a sinking on the area of the active zone. The process of the depression's forming is separatable to: widening, and deepening. A general sinking takes place at the beginning of the process, then the material loss will localize to an ever smaller part. First, deepening occurs at this part. The cause of this deepening (sinking) is the material transport and the compaction following the growth of the void volume. The sinking is inhibited by the material which gets from the passive zone to the active. By the deepening of the depression the angle of its slope are getting gradually higher. When the angle of the slopes exceed a certain value, the yet small sized depression starts to widen because the matter from it's edge moves towards the bottom of it. When this happens the deepening of the depression stops, moreover it's depth can even decrease. Every grain size has its own naturally slope angle. Thus the rate of the deepening and the widening is roughly equal in case of the cover is built with the use of the smallest grain. The almost perfect cone-shaped depressions develop in this case. When the cover is made of big grains, they move harder on each

DOI: https://doi.org/10.30564/jgr.v2i1.1988

other, thus such a depression can form which has a bigger depth compared to its width.

This process examined by us can be modified by some parameters, like the amount of water between the grains, the shape and nature of the grain etc. However these parameters were not subject to our research.

4.5 Estimating the Connection between the Size of the Subsidence Dolines and the Influencing Parameters' Sizes of Its Formation

A quotient is calculatable from the sizes (depth and diameter) of the model experiment's depression and the cover's thickness. The sizes of the model experiment's depression are a hundred times smaller than the sizes of the dolines in the nature. From the value of this quotient the cover's thickness by natural dolines is ascertainable (if their sizes are known), knowing that the size values of the natural dolines are exactly the same in meters as the values of the depression in the model experiment in centimeters. We calculated the value of this quotient with the chimney diameter of 1.5 cm so it corresponds with 1.5 m chimney diameter in the nature. The connections we analysed were the followings:

(1) the depth of the depression and the cover's thickness in its surroundings,

(2) the diameter of the depression and the cover's thickness in its surroundings.

The estimated data for the cover's thickness based on the depth of the depression are the followings:

The estimated data for the cover's thickness based on the diameter of the depression are the followings:

The values shown above (table 7 and 8) are only from the model experiment's results we presented above. Thus some influence factors which impact the size of the subsidence dolines and are present in the nature were disregarded. Such are the age of the covered karstic depressions, the area specific amount of precipitation, the character of the bedrock, the amount of CO_2 in the soil air etc. Even so these data could be good guidance in case we want to estimate the cover's thickness without using VES measurements.

5. Conclusion

According to the model experiment the influence factors of the depression's forming are the diameter and the length of the chimney, the cover's thickness, and the grain size of the cover. These parameters influence the depression's forming and the size of the occuring form, not only separately but collectively too. According to our model experiments, forming a depression has a lot of conditions. A depression can form only in that case, when all of these parameters reach a certain threshold value. Thus, from the aspect of the depression to form; small chimney diameter, big grain size, and thick cover can be unfavourable parameters. The depression of the model experiment develops on the area of the active zone by sinking. The sinking is caused by the material loss, and the compaction followed by the associated void volume growing. Knowing that our model has a 1:100 scale and the quotient of the parameters examined in the model experiment, considering the size of natural suffosion dolines', cover thickness and chimney diameter are estimable.

Table 7. Estimating the cover's thickness suggested to the depth of the depression

A depression's depth in the nature (m)	A depression's depth in the model experiment (cm)	The cover's thickness in the model experiment (cm)	The quotient of the cover's thickness and the depth of the depression by the data of the model experiment	Calculated cover thickness by the depressions in case of the declared values (m)
2.5-3	2.5-3	5	1.78	4.5-5.5
2-2.5	2-2.5	10	3.3	6.6-8.3
1.5-2	1.5-2	15	6	9-12
1-1.5	1-1.5	20	10	10-15
lesser than 1	lesser than 1	more than 20	20	more than 20

Table 8. Estimating the cover's thickness suggested to the diameter of the depression

A depression's diameter in the nature (m)	A depression's diameter in the model experiment (cm)	The cover's thickness in the model experiment (cm)	The quotient of the cover's thickness and the diameter of the depression by the data of the model experiment	Calculated cover thickness by the depressions in case of the declared values (m)
7-8	7-8	5	0.5	3.5-4
6-7	6-7	10	1.25	7.25-7.5
5-6	5-6	15	1.9	9.5-11.4
4-5	4-5	20	2.8	11.2-14
lesser than 4	lesser than 4	more than 20	5.5	more than 22

References

[1] Curl, R. L. Scallops and flutes. Transactions Cave Research Group Great Britain, 1966, 7: 121-160.

[2] Quinif, Y. Contribution a l'étude morpholoqique des coupoles. Annales de spéléologie, 1973, 28(4): 565-573.

[3] Fabre, G., Nicod, J. Lapiates, methods and role of corrosion, crypto-karst - Phenomen karst 3, Memoirs and documents of geography, 1982, 3: 115-131. (in French)

[4] Glew, J. R., Ford, D. C. Simulation study of the developement of rillenkarren. Earth Surf. Proc., 1980, 5: 25-36.

[5] Dzulinsky, S., Gil, E., Rudnicki, J. Experiments on kluftkarren and related lapis forms. Z. Geomorphology, 1988, 32 (1): 1-16.

[6] Veress, M., Pidl, K., Mantler, M. The modelling of the karstification of gypsum under laboratory circumstances. Scientific Publications of the Berzsenyi Teacher Training College in Szombathely 11. Natural Sciences, 1998, 6: 147-166. (in Hungarian)

[7] Veress, M., Péntek, K. Theoretical model of surface karstic processes. 30/5000, Journal of Geomorphology, 1996, 40(4): 461-476. (in Hungarian)

[8] Deák, Gy., Szemes, M., Veress, M. Water movements of the plaster cover on physical analogue models. Karst Development, 2015, 20: 215-229. (in Hungarian)
DOI: 10.17701/15.215-229

[9] Deák, Gy., Péntek, K., Füzesi, I., Vetési-Foith, Sz., Veress M. Modeling of the debris zone that developed during karstification. Karst Development, 2017, 22: 61-75. (in Hungarian)
DOI:10.17701/17.61-75

[10] Deák, Gy., Vetési-Foith, Sz., Péntek, K. Examination of the relationship between the depth of saturated water level and the karstic surface development by model experiments. Karst Development, 2018, 23: 31-43. (in Hungarian)
DOI: 10.17701/18.31-43

[11] Veress, M., Gárdonyi, I., Deák, Gy. The study of covered karstification on a gypsum plate with cover. Karst Development, 2014, 19: 159-171. (in Hungarian)

[12] Vetési-Foith, Sz. Examination of the subsidence dolines's with the use of model experiments. Karst Development, 2018, 23: 85-93. (in Hungarian)
DOI: 10.17701/18.85-93

[13] Arevalo, R., Zirugiel, I. Clogging of granular materials in silos: effect of gravity and outlet size. Soft Matter, 2015, 12: 123-130.
DOI: 10.1039/C5SM01599E

[15] He, K., Liu, C., Wang, S. Karst collapse related to over-pumping and a criterion for its stability. Environ Geol, 2003, 43: 720-724.

[15] Sweeting, M. M. Karst Landforms. Columbia University Press, New York, 1973.

[16] Waltham, T., Bell, F., Culshaw, M. Sinkholes and Subsidence. Springer, Berlin-Heidelberg, 2005.

[17] Currens, J. C., Paylor, R. L., Beck, E. G., Davidson, B. A method to determine cover-collapse frequency in the Western Pennyroyal karst of Kentucky. J Cave Karst Stud, 2012, 74(3): 292-299.

[18] Veress, M. Covered karsts. Springer, Berlin-Heidelberg, 2016.

[19] Waltham, A. C., Fookes, P. G. Engineering classification of karst ground conditions. Quarterly Journal Engineering Geology Hydrogeology, 2003, 36: 101-118.

[20] Williams, P. W. Dolines. In: Gunn, J. (Eds.): Encyclopedia of Caves and Karst Science. Taylor and Fitzroy Dearborn, London, New York, 2004: 304-310.

[21] Upchurch, S., Scott, T. M., Alfieri, M. C., Fratesi, B., Dobecki, T.L. Epigene and Hypogene Karst. The Karst Systems of Florida Cham, Springer, 2019: 359-441.

[22] Chen, J., Beck, B. F. Qualitative modelling of the cover-collapse process. In: Beck, B. F. (Eds.): Engineering and Environmental Impacts of Sinkholes and Karst, Balkema: Rotterdam, 1989: 98-95.

[23] Benson, R. C., Kaufmann, R. D. Characterization of a highway sinkhole within the gypsum karst of Michigan. In: Beck, B. F., Herring, J. G., (Eds.): Geotechnical and environmental applications of karst geology and hydrology. Balkema, Lisse, 2001: 103-112.

[24] Crawford, N. C. Environmental problems associated with urban development upon karst, Bowling Green, Kentucky. In: Beck, B. F., Herring, J. G. (Eds.): Geotechnical and Environmental Applications of Karst Geology and Hydrology, Balkema: Lisse, 2001: 397-424.

[25] Klimchouk, A., Andrejchuk, V. Karst breakdown mechanisms from observations in the gypsum caves of the Western Ukraine: implications for subsidence hazard assessment. Int. Speleol., 2003, 31(1/4): 55-88.

[26] Hyatt, J. A., Wilson, R., Givens, J. S., Jacobs, P. M. Topographic, geologic and hydrogeologic controls on dimension and locations of sinkholes in thick covered karst, Lowndes Country, Georgia. In: Beck, B. F., Herring, J. G. (Eds.): Geotechnical and Environmental Applications of Karst Geology and Hydrology, Balkema, Lisse, 2001: 37-45.

  DOI: https://doi.org/10.30564/jgr.v2i1.1988

BILINGUAL PUBLISHING CO.
Pioneer of Global Academics Since 1984

Journal of Geological Research
https://ojs.bilpublishing.com/index.php/jgr-a

ARTICLE

Properties of Natural Catastrophes

Ospanova N.K.*

Laboratory of paleontology and stratigraphy, Institute of Geology, Earthquake Engineering and Seismology of the National Academy of Sciences of Tajikistan, Tajikistan

ARTICLE INFO

Article history
Received: 16 June 2020
Accepted: 26 June 2020
Published Online: 30 June 2020

Keywords:
Earthquake
Biotic crises
Catastrophism
Evolution
Spontaneity
Changes

ABSTRACT

A variety of phenomena of a catastrophic order and fear of their consequences served as the reason that until now the properties of disasters remained incomprehensible. We found out the properties of natural catastrophes. It is shown that knowledge of these properties is of great importance, because it contributes to the formation of an objective judgment on natural processes and phenomena.

1. Introduction

The interest of geology and paleontology in the study of disasters is not accidental; it is due to the fact that numerous phenomena of a catastrophic nature fall into the sphere of study of these sciences. These include earthquakes, mudflows, landslides, collapses, volcanic eruptions, biotic crises and more. The mere statement of these phenomena is not the key to their knowledge, and each event requires a thorough description and study, because any catastrophe has "its own face". A variety of events of catastrophic order is the reason that in the study of catastrophes there are many unclear points regarding both their prediction and their consequences. Therefore, the question arises: are there any common features inherent in such a diverse range of phenomena?

We have clarified the properties of a catastrophe as a natural phenomenon [1,2]. But due to the vastness of the topic, we only mentioned in passing that one of the consequences of the disaster is the emergence of a new quality. Here this point is covered in more detail. This work is a continuation of earlier research.

2. Methodological Premises of the Study

When clarifying the properties of natural disasters, the author used the experience obtained as a result of many years of study of the evolution of Paleozoic corals. Despite the specifics of the development of different groups of the organic world, as well as the specifics of the evolu-

**Corresponding Author:*
Ospanova N.K.,
Laboratory of paleontology and stratigraphy, Institute of Geology, Earthquake Engineering and Seismology of the National Academy of Sciences of Tajikistan, Tajikistan;
Email: ospanova2005@mail.ru

 DOI: https://doi.org/10.30564/jgr.v2i1.2004

tion of the living and nonliving, there are general fundamental principles that equally act at different levels of the existence of matter and have power both for the functioning of biological systems and for the functioning of ordinary physical systems. Therefore, we consider the clarification of the evolutionary properties of individual groups of animals and heliolitids as one of the bricks that can be used in constructing of the General Theory of Evolution. The author took into account the mathematical approach to explaining phenomena of a catastrophic order, as well as the traditional approach to understanding catastrophes as large-scale events that entail negative consequences. The synthesis of numerous data, as well as the interest in the evolution of the organic world and evolution in general, allowed the author to establish the properties of the catastrophe as a natural phenomenon.

3. Catastrophe Properties

A wide audience, most likely, is not very familiar with our studies due to their novelty and the limited number of publications; therefore we consider it necessary to briefly recall the properties of the catastrophe that we established as a natural phenomenon. The catastrophe is understood as *a sudden change in the behavior of the system, as well as the general type of systems in which such changes occur* [3], and from these positions a huge number of phenomena fall under the definition of the catastrophe: evaporation of water, sudden tipping over or falling of an object, change of mood, differentiation of cells, the appearance of a rainbow in the sky, etc. The multidimensional nature of the disasters makes it clear that they include not only natural disasters, faults of regional significance, giant folded systems, multi-kilometer thrusts and landslides, but also micro-fractures, local displacements of rocks, small folding, even if these folds are only a few millimeters.

A catastrophe has the following properties: sudden manifestation (which follows already from its definition), relative short duration, irreversibility of consequences, unpredictability, spontaneity [1,2], and long-range action [2].

The relative short duration is due to a sharp disruption of the balance that existed before a catastrophe; because of this the energy release associated with the catastrophe is pulsed. In order for the catastrophe to occur, it is necessary to achieve a certain critical level of energy required to starting the catastrophe and overcome its resistance to the external environment, the balance of which it violates. Pulse discharge, which determines the high speed of the catastrophe, explains the short duration of its action.

Irreversibility of the consequences stems not only from the fact that the catastrophe does not fit into the surrounding course of development and violates its order, but also from the relative short duration of the catastrophe, as well as the composition of its elements. Stewart [3] identified the components of the catastrophe: *the space of control parameters, the space of variable states,* and *the response surface*. The presence of a region of variable states between the control space and the response surface causes a qualitative difference between the beginning and end of the disaster.

Unpredictability follows from the suddenness of the manifestation and can relate both to the time of the beginning or end of the catastrophe, the place of manifestation, so to its intensity, the magnitude of the impact and the evaluation of the consequences. No one can know in advance the energy potential of the catastrophe, as well as the resistance of the environment, which it overcomes and which is different in each case. Therefore, it is difficult to predict both the time of its beginning and the whole range of consequences caused by it. From this it follows that *in the matter of predicting disasters there will always be a greater or lesser area of uncertainty*.

Spontaneity is associated with the inability to prevent a catastrophe. There is a gap between the space of control parameters and the response surface in the form of the space of variable states, and intervention in the course of the catastrophe is possible only in the space of variable states. Due to the transience of the process, it is difficult to do as much as trying to stop an explosion that has already begun. Spontaneity can also manifest itself in the fact that one catastrophe is capable of provoking a cascade of catastrophes. *The cascade of catastrophes is a series of catastrophic events that follow each other*. The duration of the intervals between them depends on the specific conditions in which the disaster occurred, and can range from the first seconds and minutes to several days and months. For example, the events of 1911 in the Pamir can be reflected in the following scheme of cascade: *an earthquake - a collapse of rocks blocking the river bed - filling a reservoir with water* (the emergence of Lake Sarez). A simplified diagram of the tsunami-related cascade is as follows: *earthquake - tsunami - destruction of buildings (coastline, dams, etc.) - flood.*

In addition to these properties, long-range action is inherent in catastrophes: the remote consequences of the catastrophe are more durable than the catastrophe itself. That is, the consequences of the disaster last much longer than the time of the disaster. Such a paradox occurs due to the difference in the speed of implementation of different processes. The speed of the catastrophe itself is huge, so the inverse proportion to it - time - is small. The consequences caused by the catastrophe are less energetically saturated (if there is no replenishment with additional por-

DOI: https://doi.org/10.30564/jgr.v2i1.2004

tions of energy) and proceed at a slower rate; respectively, the time for their implementation increases. For example, impact events are short-lived, the fires, destruction and "cosmic winters" caused by them last much longer, and it may take hundreds or thousands of years to restore destroyed biocenoses. An atomic explosion lasts seconds or fractions of the second, the radioactive cloud generated by it exists for a longer period, the increased radiation field lasts for many years, and genetic abnormalities due to radiation exposure affect hundreds or thousands of generations, and so on.

Since disasters cover a huge range of phenomena, examples can be very diverse and numerous [2]. Here we would like to give only a few illustrative examples regarding the unpredictability property and related to geology.

The seismic shocks that make up the earthquake are divided into foreshocks (shocks preceding the main one), the main shock (maximum in strength) and aftershocks (shocks following the main one). Practice shows that it is very difficult to predict in advance the number of shocks that accompany the main earthquake, their strength and the possibility of occurrence. There is large number of such earthquakes, which were not accompanied by additional shocks. But there are other examples. During the Karatag earthquake (October 21, 1907), three shocks of the same strength occurred (9 points each), followed by an interval of 21 and 6 minutes. In total, 12 000 people were killed. A Garm earthquake of magnitude 8–9 occurred on April 20, 1941, and then up to April 1, 1942, about 200 seismic shocks of different strengths were noted [4]. After the main shock of the Vahdat earthquake with the magnitude of 6-7 points (November 10, 2013), from November 10 to 30, 370 aftershocks were recorded [5]. Scientists believe that the number of aftershocks can reach several thousand.

It should be noted that at present about 200 earthquake precursors are known, but not one of them can "predict" the exact time of the start of the earthquake. The same can be stated in relation to other catastrophic phenomena, for example, tsunamis. At one time, Soviet scientists set the threshold for the magnitude of Pacific underwater tremors giving rise to tsunamis. For 20 years they have not missed the single tsunami. The paradox is that three quarters of the alarms turned out to be false [6].

4. Irreversible changes

Scientists consider the unidirectionality of processes as a property of internal asymmetry inherent in nature [7]. This statement in itself is only an ascertaining of what is observed in practice, but by no means an explanation of the essence of asymmetry. From the standpoint of the properties of the catastrophe as a natural phenomenon, the asymmetry that manifests itself quite often finds its natural explanation: the high quality of the beginning and end of the catastrophe and the practical impossibility of intervening in its course due to the impulsive nature of the realization are the reasons that the previous state is replaced by the new, different from the previous one, expressed in the emergence of the new quality. Breaking the old, cardinal changes impede the restoration of the system in its previous form, both due to the fact that its elements undergo the change, as well as due to the death of some of the elements. In addition, the imbalance, as a rule, is associated with a series of events, which we call the "cascade" [1,2], when one equilibrium shift provokes the series of shifts. Therefore, as a rule, not one prohibition, but the series of prohibitions impedes the course of reverse changes. The space of variable states between the beginning and the end of what scientists understand as the catastrophe plays the role of not only the guiding channel, but also the role of the negating link - when the previous state of equilibrium is already broken, and the canalizing changes, which have begun, cannot return the system to its original state.

One of the consequences of the disaster, therefore, is the emergence of a new quality.

As a new quality, one can consider, for example, the accumulation of huge reserves of fresh water in Lake Sarez, formed as a result of the Usoi collapse, provoked by an earthquake and blocking the river [8].

A striking catastrophic event is the fall of an asteroid. Traces of the fall are recorded on space and aerial photographs in the form of ring structures, the dimensions of which allow us to judge the scale of the event. Space aliens not only left craters, but also violated the normal stratification of rocks, created high temperatures and pressures, as a result of which mineral deposits that were gigantic in their reserves could arise (the emergence of a new quality). An example is the Popigai crater in Russia (100 km, 36 million years), which is associated with the field of industrial diamonds. Scientists have calculated that they can provide all of humanity for 3 000 years in advance (oral report by Academician B.S. Zeylik). The Wredefort crater in South Africa (200km, age 2 billion years) gravitates to half of the world's gold reserves. Chicxulub in Mexico (180km, 65 Ma) is 2/3 of Mexican oil production. Finally, Sudbury in Canada (200km, 1.9 billion years old) contains 1/3 of the world's nickel reserves [9], etc.

We can also recall that after mass extinctions that have repeatedly occurred in the history of the Earth's organic development, biota never returned to its previous state: the taxonomic composition changed, ecological dominants completely changed, the nature of biotic and abiotic connections became different. Evolution began to go in a completely different way. Therefore, one geological era is not similar to another, and the division of geological time is carried out precisely on the basis of the staged development of the organic world. The qualitative difference between the different stages of the geological development of biological life can be explained from the standpoint of the properties of the catastrophe itself (impossibility of returning to the initial state). As Gould points out [10], the intensity of episodes of drastic changes establishes a hierarchy of geochronological intervals: the largest episodes serve as the boundaries of the eras (Cambrian biotic explosion, Permian and Cretaceous extinctions), and the smaller ones as the boundaries of periods.

Since the catastrophe leads to the emergence of a new quality and completely changes the direction of development, and the state of equilibrium before the catastrophe's begin differs from the state of equilibrium after catastrophe, it follows that the catastrophe leaves its mark forever. Violating the initial state of equilibrium, the disaster thereby violates the symmetry that existed before it in nature between abiotic factors or systems, between biotic ones or between those and others [2]. Regarding living things, it should be noted that the catastrophe itself does not induce organisms to change, but it changes the environment, and the changed environment, in turn, can stimulate the change of organisms.

5. Discussion

Cuvier is considered as the founder of catastrophism in geology, who proposed in 1812 the hypothesis of overturns (from the Greek *katastrophe* - overturn) expressed in interruption of long periods of stability by individual extinctions and structural disagreements. Cuvier postulated a relatively small number of disasters and spread them only on land (flooding of the islands), he did not describe any marine disasters and cataclysms. Unlike Cuvier, British researchers believed that each interval of geological time was accompanied by a catastrophe and that their total number was close to one hundred [11].Cuvier spoke of one act of creation, while the British believed that every calm interval of time ended in the cataclysm destroying all life, and then the Creator re-created the world, where other forms played a role. A sharp change in organic residues made it possible to build maps of the occurrence of layers, which over time acquired practical significance in the constructing work. Thus, although Cuvier is considered to be the founder of catastrophism, different researchers (or different scientific schools) put different meanings in the concept of catastrophe and catastrophism.

Over time, the views on catastrophes and catastrophism underwent changes - from the recognition of the global nature of catastrophes (for example, the theory of Eli de Beaumont about the collapse of the earth's crust to shrink as a result of cooling of the bowels or G. Shtille's point of view about the simultaneity of mountain formation on the whole Earth) to their denial. Gould [10], who postulated principle of intermittent change, considers the term "catastrophic" unsuccessful in relation to many important processes of the physical and biological development of the Earth; periods of sharp changes he calls “leap”. Gretener believes that the term “catastrophism” is burdened with a hint of annihilation, and it cannot be used to refer to geological events, which are simply quick changes, destructive for some and beneficial for others. He considers the terms “spasm”, “episode”, “event”, “leap”, “point change” as more neutral [12]. On the contrary, Benson sees the sharp transition between old and new species as paleontological confirmation of the presence of microcatastropism, which is a common way of evolution of species [11]. Emergy writes that in a certain sense both magmatic and metamorphic minerals can be considered catastrophic in origin, since the processes that form the primary deposits are discontinuous in time and space [13]. At the same time, he makes a reservation that these natural processes are likely to occur always in one place or another on the Earth, therefore, both primary and secondary mineral deposits can serve as examples of uniformism (uniformity theory).

It is clear from the statements of the authors that in their constructions they do not take into account mathematical achievements in relation to understanding of catastrophes.

We may not know the name of the founder of the mathematical theory of catastrophes Rene Thom; we are not required to study the theory of peculiarities of Hassler Whitney. But one cannot ignore the fact that many unrelated phenomena obey the same laws. For example, a Dovetail type catastrophe (a dovetail curve) is considered as a universal model because of the constant occurrence in the theory of peculiarities of smooth mappings. So many disasters can be portrayed with this model [14]. The catastrophe in the understanding of mathematicians is *a sudden change in the characteristics of a system with small, smooth changes in its external or internal parameters*. It is emphasized that *the crisis of the system occurs instantly*. Using this part of the mathematical analysis, a wide variety of phenomena can be described, including riots in prisons. That is, this area of theoretical research has the most immediate practical significance. Therefore, it is hardly possible to recognize as correct the ignoring of the term “catastrophe” in relation to geological phenome-

DOI: https://doi.org/10.30564/jgr.v2i1.2004

na. The terms for which Gretener [12] advocates as neutral ("spasm", "episode", "event", "leap", "point change"), due to their neutrality and semantic ambiguity, do not possess the informativeness that the word "catastrophe" has. For example, the arrow of a device can make the leap and return to its former position, which cannot be said about disasters: disrupting the existing equilibrium, they completely change the balance of forces.

At the same time, mathematical curves that describe the behavior of an object at the moment of changing its state do not reveal the essence of a catastrophe as a natural phenomenon. First, the same curve covers a wide range of unrelated phenomena. Secondly, the curves on the plane cannot give an idea of the visible damage that cause disasters in the area, as well as the consequences of these damages. Therefore, we believe that establishing the properties of the catastrophe as the natural phenomenon is important for understanding the essence of real events.

6. Conclusions

Studying the properties of a disaster helps to understand many phenomena, which simply cannot be displayed in one small article. Only the geological aspect of disasters is affected here. In particular, the reason for the difference in different stages of the geological development of the Earth is shown. Is it possible, based on the fact that catastrophes lead to the emergence of a new quality, to draw a conclusion about the creative role of catastrophes? No, the catastrophe is always destruction, it plays the role of closed doors, putting a ban on certain areas of development and thereby channeling the choice of another development way. As stated above, the catastrophe does not induce organisms to change, but it changes the environment, and the changed environment, in turn, can stimulate a change in the living.

An analysis of the nature of the catastrophic changes shows that in the matter of catastrophe prediction there always remains a greater or lesser area of uncertainty. Nevertheless, one often hears undeserved accusations against scientists about the fact that they still "have not learned" to predict the exact time of the start of an earthquake. Moreover, the scientists themselves are also lamenting about this. Such a philistine point of view is based on absolute ignorance of the properties of natural catastrophes. In the case of disasters, we are dealing with statistical, averaged data, and not with accurate. For example, some leading scientists consider the frequency of seismic activity as a very dubious forecast criterion [15]. Any events in this world have the probabilistic nature of implementation, and the probability can change over time.

We borrowed a mathematical definition of a catastrophe and its elements. But it is clear that the study of the properties of disasters cannot be limited by mathematical curves because they do not cover the whole spectrum of concomitant changes caused by disasters, and do not provide a visual representation of real events.

Elucidation of the properties of a catastrophe aims to form an objective view of natural processes and phenomena. The study shows that false hopes of the exact time prediction of the beginning of disasters must be discarded. This does not mean that it makes no sense to identify the precursors of earthquakes, volcanic eruptions or tsunamis; we must study the world in which we live. But sometimes illusions can be just as harmful as ignoring the obvious facts.

References

[1] Ospanova, N.K. Catastrophes as an integral property of the geodynamic development of the Earth[M]. Geodynamics, mineralization and geoecological problems of the Tien Shan: Materials of the International Conference on the 70th anniversary of the Institute of Geology of the National Academy of Sciences of the Kyrgyz Republic (September, 2013). Bishkek: Ilim. 2013: 167-172.

[2] Ospanova, N.K. Anthropogenic factors in the light of the doctrine of natural catastrophes[J]. The scientific heritage. Budapest, 2020, 2(45): 24-30.

[3] Stewart, J. Secrets of the catastrophe[M]. Moskow: Mir. 1987: 76.

[4] Niyazov, Dj.B. Garm earthquake of 1941 and the beginning of the establishment of the seismic service of Tajikistan[M]. Geology and issues of seismicity of the territory of Tajikistan (Materials of a scientific conference dedicated to the 80th anniversary of Academician of the Academy of Sciences of the Republic of Tatarstan, Doctor of Geological and Mineralogical Sciences Djalilov Manzur Rakhimovich). Dushanbe: Balogat. 2014: 218-219.

[5] Djuraev, R.U. Geological aspects of the Wahdat earthquake on November 10, 2013[M]. Problems of geology, seismology and earthquake engineering of Tajikistan (Materials of the Republican conference dedicated to the 30th anniversary of the Kairakkum earthquake on October 13, 1985. Dushanbe: Sadoi Kalb. 2016: 190-195.

[6] Aristarchov, N. Understand and predict[J]. Knowledge is power. 1985(8): 9-10.

[7] Atkins, P.W. Order and disorder in nature[M]. Moscow: Mir. 1987: 234.

[8] Shpilko, G.A. The 1911 earthquake in the Pamirs and its consequences[M]. St. Petersburg. 1914: 94.

[9] Zeylik, B.S. The problem of space protection to save life on the planet and where to look for mineral deposits[M]. Geology in the XXI century: Materials of the International scientific-practical conference "Satpayev readings" dedicated to the 20th anniversary of independence of the Republic of Kazakhstan (Almaty, April 14-15, 2011). Almaty: IP Volkova N.A. 2011: 85-91.

[10] Gould, S.J. In defense of the concept of intermittent change[M]. The New Uniformitarianism / W.A. Berggren and John A. van Convering (Eds.). Moscow: Mir. 1986: 13-41.

[11] Benson, R.H. Completeness, Continuity, and Common Sense in Historical Geology[M]. Catastrophes and Earth History. The New Uniformitarianism / W.A. Berggren and John A. van Convering (Eds.). Moscow: Mir. 1986: 42-88.

[12] Gretener, P.I. Reflections on a “rare event” and related representations in geology[M]. Catastrophes and Earth History. The New Uniformitarianism / W.A. Berggren and John A. van Convering (Eds.). Moscow: Mir. 1986: 89-100.

[13] Emergy, K.O. Catastrophes and the Modern World[M]. Catastrophes and Earth History. The New Uni-formitarianism / W.A. Berggren and John A. van Convering (Eds.). Moscow: Mir., 1986: 444-456.

[14] Arnold, V.I. Catastrophe theory[J]. Science and life. 1988, 10: 12-19.

[15] Waltham, T. Catastrophe: the violent Earth[M]. Leningrad: Nedra. 1982: 223.

  DOI: https://doi.org/10.30564/jgr.v2i1.2004

Author Guidelines

This document provides some guidelines to authors for submission in order to work towards a seamless submission process. While complete adherence to the following guidelines is not enforced, authors should note that following through with the guidelines will be helpful in expediting the copyediting and proofreading processes, and allow for improved readability during the review process.

Ⅰ. Format

- Program: Microsoft Word (preferred)
- Font: Times New Roman
- Size: 12
- Style: Normal
- Paragraph: Justified
- Required Documents

Ⅱ. Cover Letter

All articles should include a cover letter as a separate document.

The cover letter should include:

- Names and affiliation of author(s)

The corresponding author should be identified.

Eg. Department, University, Province/City/State, Postal Code, Country

- A brief description of the novelty and importance of the findings detailed in the paper

Declaration

v Conflict of Interest

Examples of conflicts of interest include (but are not limited to):

- Research grants
- Honoria
- Employment or consultation
- Project sponsors
- Author's position on advisory boards or board of directors/management relationships
- Multiple affiliation
- Other financial relationships/support
- Informed Consent

This section confirms that written consent was obtained from all participants prior to the study.

- Ethical Approval

Eg. The paper received the ethical approval of XXX Ethics Committee.

- Trial Registration

Eg. Name of Trial Registry: Trial Registration Number

- Contributorship

The role(s) that each author undertook should be reflected in this section. This section affirms that each credited author has had a significant contribution to the article.

1. Main Manuscript
2. Reference List
3. Supplementary Data/Information

Supplementary figures, small tables, text etc.

As supplementary data/information is not copyedited/proofread, kindly ensure that the section is free from errors, and is presented clearly.

Ⅲ. Abstract

A general introduction to the research topic of the paper should be provided, along with a brief summary of its main results and implications. Kindly ensure the abstract is self-contained and remains readable to a wider audience. The abstract should also be kept to a maximum of 200 words.

Authors should also include 5-8 keywords after the abstract, separated by a semi-colon, avoiding the words already used in the title of the article.

Abstract and keywords should be reflected as font size 14.

Ⅳ. Title

The title should not exceed 50 words. Authors are encouraged to keep their titles succinct and relevant.

Titles should be reflected as font size 26, and in bold type.

Ⅳ. Section Headings

Section headings, sub-headings, and sub-subheadings should be differentiated by font size.

Section Headings: Font size 22, bold type

Sub-Headings: Font size 16, bold type

Sub-Subheadings: Font size 14, bold type

Main Manuscript Outline

Ⅴ. Introduction

The introduction should highlight the significance of the research conducted, in particular, in relation to current state of research in the field. A clear research objective should be conveyed within a single sentence.

Ⅵ. Methodology/Methods

In this section, the methods used to obtain the results in the paper should be clearly elucidated. This allows readers to be able to replicate the study in the future. Authors should ensure that any references made to other research or experiments should be clearly cited.

Ⅶ. Results

In this section, the results of experiments conducted should be detailed. The results should not be discussed at length in this section. Alternatively, Results and Discussion can also be combined to a single section.

Ⅷ. Discussion

In this section, the results of the experiments conducted can be discussed in detail. Authors should discuss the direct and indirect implications of their findings, and also discuss if the results obtain reflect the current state of research in the field. Applications for the research should be discussed in this section. Suggestions for future research can also be discussed in this section.

Ⅸ. Conclusion

This section offers closure for the paper. An effective conclusion will need to sum up the principal findings of the papers, and its implications for further research.

Ⅹ. References

References should be included as a separate page from the main manuscript. For parts of the manuscript that have referenced a particular source, a superscript (ie. [x]) should be included next to the referenced text.

[x] refers to the allocated number of the source under the Reference List (eg. [1], [2], [3])

In the References section, the corresponding source should be referenced as:

[x] Author(s). Article Title [Publication Type]. Journal Name, Vol. No., Issue No.: Page numbers. (DOI number)

Ⅺ. Glossary of Publication Type

J = Journal/Magazine

M = Monograph/Book

C = (Article) Collection

D = Dissertation/Thesis

P = Patent

S = Standards

N = Newspapers

R = Reports

Kindly note that the order of appearance of the referenced source should follow its order of appearance in the main manuscript.

Graphs, Figures, Tables, and Equations

Graphs, figures and tables should be labelled closely below it and aligned to the center. Each data presentation type should be labelled as Graph, Figure, or Table, and its sequence should be in running order, separate from each other.

Equations should be aligned to the left, and numbered with in running order with its number in parenthesis (aligned right).

Ⅻ. Others

Conflicts of interest, acknowledgements, and publication ethics should also be declared in the final version of the manuscript. Instructions have been provided as its counterpart under Cover Letter.

Journal of Geological Research

Aims and Scope

Journal of Geological Research publishes original research papers that offers a rapid review and publication that freely disseminates research findings in all areas of Geology including Petrology, Mineralogy, Engineering Geology, Regional Geology and more. The Journal focuses on innovations of research methods at all stages and is committed to providing theoretical and practical experience for all those who are involved in these fields.

Journal of Geological Research aims to discover innovative methods, theories and studies in all aspects of Geology by publishing original articles, case studies and comprehensive reviews.

The scope of the papers in this journal includes, but is not limited to:

- Petrology
- Mineralogy
- Geochemistry
- Stratigraphy
- Deposit Geology
- Structural Geology
- Economic Geography
- Hydrogeology
- Engineering Geology
- Regional Geology

Bilingual Publishing Co. (BPC)

Tel:+65 65881289

E-mail:contact@bilpublishing.com

Website:www.bilpublishing.com

About the Publisher

Bilingual Publishing Co. (BPC) is an international publisher of online, open access and scholarly peer-reviewed journals covering a wide range of academic disciplines including science, technology, medicine, engineering,education and social science. Reflecting the latest research from a broad sweep of subjects, our content is accessible worldwide – both in print and online.

BPC aims to provide an analytics as well as platform for information exchange and discussion that help organizations and professionals in advancing society for the betterment of mankind. BPC hopes to be indexed by well-known databases in order to expand its reach to the science community, and eventually grow to be a reputable publisher recognized by scholars and researchers around the world.

BPC adopts the Open Journal Systems, see on http://ojs.bilpublishing.com

Database Inclusion

Asia & Pacific Science Citation Index

Creative Commons

China National Knowledge Infrastructure

Google Scholar

Crossref

MyScienceWork

BILINGUAL
PUBLISHING CO.
Pioneer of Global Academics Since 1984

Tel:+65 65881289
E-mail:contact@bilpublishing.com
Website:www.bilpublishing.com